FORCED VIBRATION ANALYSIS OF GENERALLY LAMINATED COMPOSITE BEAMS USING DOMAIN BOUNDARY ELEMENT METHOD

A THESIS SUBMITTED TO
THE GRADUATE SCHOOL OF NATURAL AND APPLIED SCIENCES
OF
MIDDLE EAST TECHNICAL UNIVERSITY

BY

ZUBAIR AHMED

IN PARTIAL FULFILLMENT OF THE REQUIREMENTS
FOR
THE DEGREE OF MASTER OF SCIENCE
IN
MECHANICAL ENGINEERING

AUGUST 2018

Approval of the thesis:

FORCED VIBRATION ANALYSIS OF GENERALLY LAMINATED COMPOSITE BEAMS USING DOMAIN BOUNDARY ELEMENT METHOD

submitted by **Zubair Ahmed** in partial fulfillment of the requirements for the degree of **Master of Science in Mechanical Engineering**, **Middle East Technical University** by,

Prof. Dr. Halil Kalıpçılar
Dean, Graduate School of **Natural and Applied Sciences** _____

Prof. Dr. M. A. Sahir Arıkan
Head of Department, **Mechanical Engineering** _____

Prof. Dr. Serkan Dağ
Supervisor, **Mechanical Engineering Dept., METU** _____

Examining Committee Members

Assist. Prof. Dr. Gökhan Özgen
Mechanical Engineering Dept., METU _____

Prof. Dr. Serkan Dağ
Mechanical Engineering Dept., METU _____

Assist. Prof. Dr. Mehmet Bülent Özer
Mechanical Engineering Dept., METU _____

Assist. Prof. Dr. Ulaş Yaman
Mechanical Engineering Dept., METU _____

Assist. Prof. Dr. Reza Aghazadeh
Mechatronics Engineering Dept., THK Üni. _____

Date: 27/08/2018

I hereby declare that all information in this document has been obtained and presented in accordance with academic rules and ethical conduct. I also declare that, as required by these rules and conduct, I have fully cited and referenced all material and results that are not original to this work.

Name, Last name : Zubair, Ahmed

Signature : _____

ABSTRACT

FORCED VIBRATION ANALYSIS OF GENERALLY LAMINATED COMPOSITE BEAMS USING DOMAIN BOUNDARY ELEMENT METHOD

Ahmed, Zubair
M.S., Department of Mechanical Engineering
Supervisor : Prof. Dr. Serkan Dağ

August 2018, 75 pages

Forced dynamic response of generally laminated composite beam is analyzed by boundary element method. Static fundamental solutions are used as weight functions in the weighted residual statements. The use of static fundamental solutions gives rise to a new formulation named as Domain Boundary Element Method. Displacement field of the generally laminated composite beam is written in accordance with first order shear deformation theory and equations of motion are derived using Hamilton's principle. Developed formulation includes the Poisson's effect as well as influence of rotary inertia and shear deformation. Bending, extensional and torsional response couplings, due to orthotropic nature of the problem, are included in the formulation. Domain integrals, in the integral formulation of the problem, are evaluated by discretizing the domain and using interpolation functions. Houbolt method is used for solving the resulting system of

equations. Dynamic response, obtained via Houbolt method, is verified by comparison with analytical solution available for an homogeneous isotropic Timoshenko beam. Dynamic response of generally laminated composite beams is studied under the action of time based excitations such as concentrated step, harmonic, impulsive and uniformly distributed step loads. Influences of fiber angle in each lamina and stacking arrangement on temporal variation of deflections and longitudinal normal stress have been studied in parametric analyses. It has been demonstrated that the developed technique is an accurate and effective alternative for forced vibration analysis of generally laminated composites.

Keywords: Forced Vibration, Dynamic Analysis, Generally laminated composite beam, Domain Boundary Element Method

ÖZ

KATMANLI KOMPOZİT KİRİŞLERİN SINIR ALAN ELEMANLARI METODU YARDIMIYLA ZORLANMIŞ TİTREŞİM ANALİZİ

Ahmed, Zubair
Yüksek Lisans, Makina Mühendisliği Bölümü
Tez Yönetcisi : Prof. Dr. Serkan Dağ

Ağustos 2018, 75 sayfa

Katmanlı kompozit kirişlerin zorlanmış dinamik analizleri sınır alan elemanları metodu ile yapılmıştır. Statik temel çözümler, ağırlıklandırılmış artık ifadesinde ağırlık fonksiyonları olarak kullanılmıştır. Statik temel çözümlerin kullanımı yeni bir hesaplama yöntemi olan sınır alan elamanları metodu adı verilen yeni bir yöntemin ortaya çıkmasını sağlamıştır. Katmanlı kompozit kirişlerin sehimleri birinci mertebeden kayma deformasyonu teorisine ve Hamilton yönteminden türetilen hareket denklemlerine uygun olarak çıkartılmıştır. Geliştirilen formülasyon dönel atalet ve kayma deformasyonunun yanında Poisson etkisini de içermektedir. Eğilme, uzama ve burulma cevaplarının problemin ortotropik doğası sonucu bir araya gelmesi de hesaplamalara dahil edilmiştir. Problemin integral hesaplamalarında kullanılan alan integralleri ayrıklaştırılmış alanlar ve interpolasyon fonksiyonlarının kullanımı ile elde edilmiştir. Sistem denklemleri

Houbolt metodu ile çözülmüştür. Houbolt metodu yardımıyla elde edilen dinamik sistem cevabı homojen izotropik Timoshenko kiriş teorisi için geçerli olan analitik çözümlerle karşılaştırılarak doğrulanmıştır. Katmanlı kompozit kirişlerin dinamik cevabı noktasal step, harmonik, impulsif ve yayılı step yükleri gibi zamana bağlı yükler altında incelenmiştir. Her katmanın fiber açılarının etkisi ve sehimlerdeki geçici değişim ile eksenel normal gerilmeler parametrik analizlerle incelenmiştir. Şunulan bu yöntem katmanlı kompozitlerin zorlanmış titreşimlerinin incelenmesinde doğru ve etkili bir alternatif olarak ortaya çıkmaktadır.

Anahtar Kelimeler: Zorlanmış Titreşim, Dinamik Analiz, Katmanlı Kompozit Kiriş, Sınır Alan Elemanları Methodu

To my parents and family.

ACKNOWLEDGEMENTS

I would like to express my deepest gratitude to my supervisor Prof. Dr. Serkan Dağ for his continued guidance, advice, encouragement and insight throughout the course of this research.

I would also like to thank the jury members for their constructive comments and suggestions.

Finally, I would like to thank my family for their constant encouragement, love and support during this period.

TABLE OF CONTENTS

LIST OF TABLES

LIST OF FIGURES

LIST OF SYMBOLS

b	Width
E	Modulus of Elasticity
h	Height
k_s	Shear Correction Factor
L	Length
M_x, M_{xy}	Moment resultants
N_x	Longitudinal force resultant
Q_{xz}	Shear force resultant
q	Applied Load
u_x	Displacement component in *x*-direction
u_y	Displacement component in *y*-direction
u_z	Displacement component in *z*-direction
ϕ	Shape function
ψ_x	Rotation of transverse normal about *y* direction
ψ_y	Rotation of transverse normal about *x* direction
ε_{xx}	Longitudinal normal strain
ε_x^0	Longitudinal midplane strain
γ_{ij}	Engineering shear strain
σ_{xx}	Longitudinal normal stress
κ_x	Bending curvature
κ_{xy}	Twist curvature
ρ	Mass density

CHAPTER 1

INTRODUCTION

1.1. Composites Overview

The term composite material refers to a class of materials, in which two or more individual materials are combined in order to obtain a new material having different characteristics from its constituents. Individual components are combined such that they remain distinct in the final structure. Resulting structure has better performance characteristics as compared to its constituents acting alone. The flexibility of being engineered as per application requirement renders composite materials an attractive choice in design of different mechanical and aerospace structures.

In aviation industry, composite materials have been used for manufacturing secondary structures for many years but currently, due to advancement in composite manufacturing and maintenance techniques, composites are also used for manufacturing primary structure of aircrafts. They are preferred in automotive industry because of their high strength to weight ratio, superior crash performance and recyclability. Renewable energy sector, sports and marine industry are other notable application areas of composites.

Composite structures mostly consist of basic structural elements such as beams, plates, and shells. Beam is a one dimensional element i.e. one dimension is large as compared to other two and is suitable for carrying bending loads. Laminated composite beams (LCBs) are composed of different individual laminas glued together. Material properties of a lamina are orthotropic in nature. Based on the alignment of principal material axes with natural body axes, LCBs can be classified into two categories. LCBs are termed as specially orthotropic if natural and

principal material axes are aligned. If principal material and natural body axes are not coincident then they are termed as generally orthotropic.

Mechanics of composite materials is more involved as compared to isotropic materials and accurate prediction of response under external forces is of fundamental importance when designing a composite for a specific application. Stacking sequence, thickness and orientation angle of fibers in each lamina have a significant effect on the response to external excitations. Experimental determination of response characteristics is unfeasible due to its high cost. In order to save the time and cost associated with experimental testing and due to composite materials' involved mechanics, accurate and efficient numerical solution procedures are required for optimized design of generally laminated composites.

1.2. Literature Survey

Boundary Element Method (BEM) encompasses a group of numerical techniques where fundamental solutions, of governing equations of the problem, are employed as weight functions. BEM has several variants for instance Domain BEM, Time Domain BEM and Dual Reciprocity BEM etc. These variants arise due to difference in type of fundamental solutions and techniques of evaluation of domain integrals in the integral form of a given problem. The technique developed here for forced vibration analysis of LCBs is Domain BEM (D-BEM). In this variant of BEM, fundamental solutions are static in nature. By using these time independent fundamental solutions in weighted residual statements, integral form of the governing PDEs is obtained as a result. Houbolt method is used for approximation of time derivatives of unknown primary variables. Use of static fundamental solution results in decreased simulation time and enhanced stability characteristics [1].

Numerous studies can be found in the literature regarding composite materials. The survey presented here will focus on the application of D-BEM to various dynamic analysis problems and analysis of generally laminated composite beams including both free and forced vibrations. D-BEM has been employed for studying various dynamic problems. In a study by Carrer et al. [1], homogeneous isotropic

Timoshenko beam, having four types of classical boundary conditions, was analyzed. They studied the dynamic response of transverse deflection under the action of time dependent loads. Dynamic response obtained through D-BEM was validated by comparing it with an analytical solution for a pinned-pinned beam. For fixed-fixed and fixed-pinned cases, D-BEM solution was verified by comparison with dynamic response obtained from Finite Difference Method (FDM). CPU time comparison was carried out and D-BEM was shown to be computationally efficient than FDM in case of point step, point harmonic and distributed step loads.

Eshraghi and Dag [2] developed D-BEM formulation for functionally graded Timoshenko beams. Functionally Graded Material (FGM) beam was composed of Aluminum and Silicon Carbide (SiC). Characteristic material properties were function of the depth and Mori-Tanaka micromechanics model was used for the calculation of Poisson's ratio and Elastic modulus. Elastodynamics of fixed-fixed and pinned-pinned configurations of FGM beam, subjected to time dependent loads, was studied. Ceramic volume fraction was varied using a power function and its effect on the time history results of longitudinal normal stress and transverse deflection were analyzed.

Hatzigeorgiou and Beskos [3] proposed a D-BEM formulation for analyzing the response of 3D elasto-plastic solids subjected to dynamic excitations. They used steady state Kelvin fundamental solutions as weight functions and performed discretization of the whole domain. Houbolt method was employed for evaluation of time derivatives. A number of sample problems were analyzed and the accuracy of developed method was demonstrated by comparison with established results in the literature.

In a study of thin elastoplastic flexural plates under the action of lateral loads, Providakis and Beskos [4] employed D-BEM for investigating the dynamic response while keeping the boundary conditions arbitrary. Boundary and interior region were discretized using Quadratic isoparametric elements. Numerical results obtained from the method were compared to those found by Finite Element Method for demonstration of accuracy. Soares Jr. et al. [5] demonstrated iterative coupling

of D-BEM with Time Domain Boundary Element Method (TD-BEM). Domain was partitioned into two parts and problem was solved independently in each part. D-BEM was used to model the nonlinear part of the problem and proposed scheme was validated by solution of two example problems.

Two dimensional wave propagation problems in elastic media were studied by Carrer et al. in [6] & [7]. Approximation of time derivatives was performed using both Houbolt and Newmark methods. A comparison study was performed and applicability of Newmark method to solution of D-BEM system of equations was demonstrated. Mathematical formulation was developed for inclusion of non-homogeneous initial conditions. In a study by Providakis [8], D-BEM was used for analyzing dynamic response of elasto-plastic thick plates resting on a deformable foundation. Winkler model was used for simulating the interaction between the plate and boundary. Investigation of heat diffusion phenomena in homogeneous and isotropic media, using D-BEM, was investigated by Pettres et al. [9]. Oyarzun et al. [10] employed D-BEM for investigating the scalar wave equation problem and introduced a new time marching technique, in which Green's functions were calculated explicitly.

Due to increasing demand and use of composite structures in various industries, their dynamic response prediction has been the subject of intense research. Banerjee and Williams [11] formulated a dynamic stiffness matrix method for analyzing the free vibration problem of composite beams. In a study of free vibration problem of composite and deep sandwich beams, Marur and Kant [12] employed higher order beam theory and investigated the effect of boundary conditions on the natural frequencies. Free vibration characteristics of generally laminated composite Timoshenko beams, using dynamic FEM, were studied by Jun et al. [13]. Free vibration problem of layered composite beam, having arbitrary layup configurations, was studied by Teboub and Hajela [14] through symbolic computations. Yildirim et al. [15] modeled generally laminated symmetric composite beams according to Euler-Bernoulli and Timoshenko beam theories and compared the in-plane natural frequencies obtained from both models. In a study of layered beams, Chen et al. [16] proposed a new approach, for analyzing free

vibrations, based on the foundation of two dimensional elasticity. Jun et al. [17] investigated the free vibration response of generally layered composite beam under the action of axial point force. Their formulation was based on a higher order beam theory and exact vibration analysis was carried out using dynamic stiffness method. In a study of laminated beams by Shao et al. [18], formulation was based on higher order shear deformation beam theory and method of reverberation ray matrix (MRRM) was employed for investigating their free vibration characteristics. Yan et al. [19] used Carrera Unified Formulation (CUF) to obtain an accurate 1d model for analyzing free vibration characteristics of a pinned-pinned beam. Exact analytical solutions were obtained as a result and commercial FEM codes were used to validate the proposed method. Jafari-Talookolaei et al. [20] obtained analytical solutions for natural frequencies and mode shapes of generally laminated composite beams by using Lagrange multipliers method. Previously published results in the literature were used for comparison to validate the analytical solutions.

In a research study by Çalım [21], dynamic response of layered composite beams having non-uniform cross-sections was analyzed. Analysis was performed in Laplace domain and in order to obtain the dynamic stiffness matrix, complementary functions method was used to numerically solve the equations. Both free and forced vibration response was analyzed. Influence of non-uniformity, material anisotropy and fiber angle was investigated in the parametric analysis. In a study regarding non-linear vibration and damping analysis by Youzera et al. [22], Galerkin technique was coupled with harmonic balance method for a pinned-pinned beam. They calculated the damping parameters and performed forced vibration analysis of laminated composite beam. In parametric analysis, they examined the effects of change in material properties and geometry of LCB. In a study of thin-walled LCBs, Machado and Cortínez [23] investigated their dynamic stability under the action of transverse loading. They determined the resonance frequencies and instability regions from Mathieu equation using Hsu's procedure. Effects of fiber angle, load height, beam dimensions and approximations to geometric non-linearity on the results were analyzed. In a study of unsymmetric LCBs, Kadivar and Mohebpour [24] studied their dynamic characteristics in response to moving

external excitation. They employed FEM, with each element having 24 degrees of freedom, for studying the dynamic response and validated their approach by comparing the response of an isotropic beam with analytical solution. They carried out further analyses by varying the lay-up configuration and fiber angles of LCB.

Bahmyari et al. [25] used FEM for studying the dynamic response of inclined LCBs under the action of moving distributed loads based on both Timoshenko beam theory and Classical lamination theory (CLT). They used Newmark's method for solving the system of equations and studied the influence of layer stacking sequence, distributed load length, fiber angle, inclination angle and mass on the response of LCB. In a study involving LCB moving in axial direction, Li et al. [26] investigated its time based non-linear response under the action of blast loads in temperature dependent environment. They used large displacement theory and Galerkin procedure for obtaining equilibrium and differential equations. Parametric study was performed to analyze the influence of thermal environment, longitudinal velocity and type of blast load on the response of LCB. Tao et al. [27] studied fiber metal laminated beams' non-linear dynamic response to moving excitations in thermal environment. Equations of motion of the problem were based on Euler-Bernoulli beam theory and Von Karman geometric non-linear theory. Main focus of their analysis was the observation of change in dynamic response with variation in temperature, load velocity, material properties and geometric non-linearity. In a study of composite Timoshenko beam having two layers, Hou and He [28] employed differential quadrature method for performing its static and dynamic analyses. Results obtained were validated by comparison with FEM. Further comparison studies were carried out to show the superiority of developed scheme over FEM in calculating natural frequencies and static response of LCB.

1.3. Objective & Approach

Main purpose of the undertaken study is to develop Domain Boundary Element Method (D-BEM) formulation for forced vibration analysis of generally laminated composite beams. Equations of motion of the problem are derived using first order shear deformation theory. Steady-state fundamental solutions are found for the non-

homogeneous reduced form of governing equations, which are then used as weight functions in the weighted residual statements. Evaluation of the weighted residual statement results in integral form of the governing differential equations of the problem. System of ordinary differential equations containing time derivatives is obtained after employing discretization of the domain using quadratic cells and is solved using Houbolt method.

Developed numerical procedure is validated by comparing its results with analytical solutions available for a homogeneous isotropic beam. Dynamic response of generally laminated composite beam is studied under harmonic, concentrated step, uniformly distributed step and impulsive loads. Convergence studies are performed for demonstrating the numerical accuracy of the developed procedure.

Intention of the undertaken endeavor is providing a new formulation for better design and optimization studies of generally laminated composite beams.

1.4. General Outline

Constitutive equations of laminated composite beam and derivation of governing equations of motion are described in chapter 2.

Chapter 3 focuses on the static fundamental solutions of all governing equations. Stepwise procedure of Domain Boundary Element Method is also explained in this chapter.

Chapter 4 includes the validation of results obtained from current numerical technique by comparison with analytical solution. Parametric analyses, involving different configurations of laminated composite beam, are also described in this chapter.

Summary of findings in current study and future research directions are mentioned in Chapter 5.

CHAPTER 2

GOVERNING EQUATIONS OF MOTION

Geometry of the generally laminated composite beam, having a rectangular cross-section, analyzed in this study is shown in Fig. 1. Several unidirectional laminas are joined together to form LCB with the assumption that bonding between all layers is perfect. Hence there is no relative motion between any two layers. Length and width of LCB are represented by L and b. h is the height of LCB and its value is equal to sum of all individual layer thicknesses. x-z plane is used to study the beam's response to external excitations where *x-axis* is coincident with longitudinal axis of the beam and *z-axis* is the transverse direction in which loads are applied.

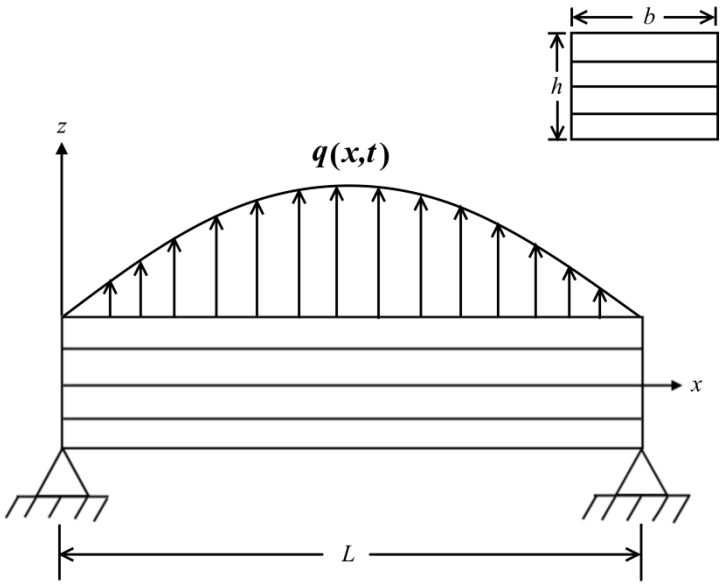

Figure 1: Generally laminated composite beam

2.1. Displacement Field

Deformation of the generally laminated composite beam is studied in accordance with Timoshenko beam theory which leads to the following displacement field

$$u_x(x,z,t) = u(x,t) + z\psi_x(x,t) \tag{1a}$$

$$u_y(x,z,t) = z\psi_y(x,t) \tag{1b}$$

$$u_z(x,z,t) = w(x,t) \tag{1c}$$

Displacements in the *x*-, *y*-, and *z*-directions are denoted by u_x, u_y and u_z. Midplane's longitudinal and transverse displacements are represented by *u* and *w*, where ψ_y and ψ_x represent the rotations of normal to the midplane about *x* and *y* axes, respectively.

2.2. Strain Displacement Relations

According to small strain theory, non-zero strains resulting from the current displacement field are given as follows

$$\varepsilon_{xx} = \frac{\partial u}{\partial x} + z\frac{\partial \psi_x}{\partial x} \tag{2a}$$

$$\gamma_{xz} = \psi_x + \frac{\partial w}{\partial x} \tag{2b}$$

$$\gamma_{xy} = z\frac{\partial \psi_y}{\partial x} \tag{2c}$$

ε_x^0, κ_x and κ_{xy} are defined as midplane strain in longitudinal direction, bending curvature and twisting curvature respectively and given as

$$\varepsilon_x^0 = \frac{\partial u}{\partial x} \tag{3a}$$

$$\kappa_x = \frac{\partial \psi_x}{\partial x} \tag{3b}$$

$$\kappa_{xy} = \frac{\partial \psi_y}{\partial x} \tag{3c}$$

2.3. LCB Constitutive Relations

For generally laminated composite beam, force and moment resultants are related to curvatures and strains through the following equations [13, 20]

$$\begin{Bmatrix} N_x \\ M_x \\ M_{xy} \end{Bmatrix} = \begin{bmatrix} \overline{A}_{11} & \overline{B}_{11} & \overline{B}_{16} \\ \overline{B}_{11} & \overline{D}_{11} & \overline{D}_{16} \\ \overline{B}_{16} & \overline{D}_{16} & \overline{D}_{66} \end{bmatrix} \begin{Bmatrix} \varepsilon_x^0 \\ \kappa_x \\ \kappa_{xy} \end{Bmatrix} \tag{4}$$

and

$$Q_{xz} = \overline{A}_{55}\gamma_{xz} \tag{5}$$

where in-plane longitudinal force, bending moment, torsional moment and shear force are represented by N_x, M_x, M_{xy} and Q_{xz} respectively. Stiffness constants in Eqs. (4) & (5) are given by [13, 29]

$$\begin{bmatrix} \overline{A}_{11} & \overline{B}_{11} & \overline{B}_{16} \\ \overline{B}_{11} & \overline{D}_{11} & \overline{D}_{16} \\ \overline{B}_{16} & \overline{D}_{16} & \overline{D}_{66} \end{bmatrix} = \begin{bmatrix} A_{11} & B_{11} & B_{16} \\ B_{11} & D_{11} & D_{16} \\ B_{16} & D_{16} & D_{66} \end{bmatrix} - \begin{bmatrix} A_{12} & A_{16} & B_{12} \\ B_{12} & B_{16} & D_{12} \\ B_{26} & B_{66} & D_{26} \end{bmatrix} * \begin{bmatrix} A_{22} & A_{26} & B_{22} \\ A_{26} & A_{66} & B_{26} \\ B_{22} & B_{26} & D_{22} \end{bmatrix}^{-1} * \begin{bmatrix} A_{12} & A_{16} & B_{12} \\ B_{12} & B_{16} & D_{12} \\ B_{26} & B_{66} & D_{26} \end{bmatrix}^{\mathrm{T}} \tag{6}$$

$$\overline{A}_{55} = k_s \int_{-h/2}^{h/2} \overline{Q}_{55} dz \tag{7}$$

where A_{ij}, B_{ij} and D_{ij} (i, j = 1, 2, 6) are components of ABD matrix of composite laminate. A_{ij} and D_{ij} represent the extensional and bending stiffness matrices whereas the B_{ij} denote the bending-extension coupling. The matrix stiffness constants and transverse shear stiffness $\overline{A}_{55}$ can be calculated as [20, 29]

$$A_{ij} = \sum_{k=1}^{n} \overline{Q}_{ij}^{k} (z_k - z_{k-1}) \qquad (i, j = 1, 2, 6) \tag{8a}$$

$$B_{ij} = \frac{1}{2}\sum_{k=1}^{n} \overline{Q}_{ij}^{k}(z_k^2 - z_{k-1}^2) \qquad (i, j = 1, 2, 6) \qquad (8b)$$

$$D_{ij} = \frac{1}{3}\sum_{k=1}^{n} \overline{Q}_{ij}^{k}(z_k^3 - z_{k-1}^3) \qquad (i, j = 1, 2, 6) \qquad (8c)$$

$$\overline{A}_{55} = \sum_{k=1}^{n} k_s \overline{Q}_{55}^{k}(z_k - z_{k-1}) \qquad (8d)$$

In the above equations, superscript *k* indicates layer number and *n* is total number of layers. Layer coordinates of the k^{th} lamina from the geometric midplane of LCB are denoted by z_k and z_{k-1}. Figs. 2 and 3 show fiber angle in an individual lamina and layer coordinates in LCB, respectively.

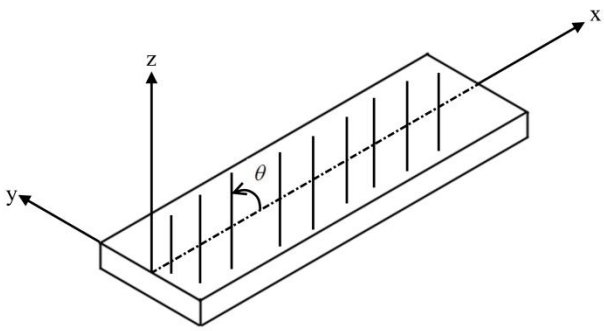

Figure 2: Fiber angle orientation

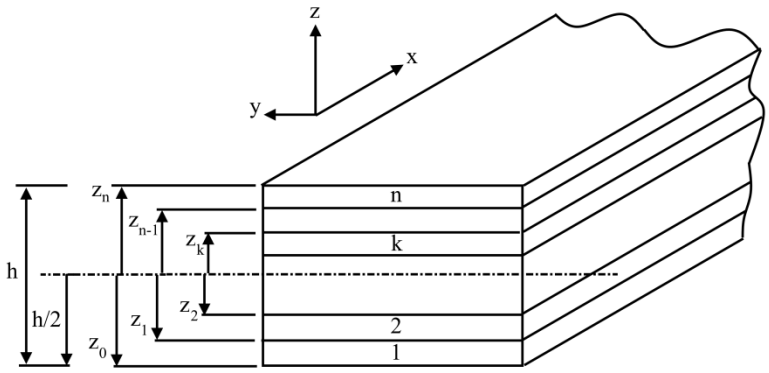

Figure 3: Layer coordinates

k_s is the shear correction factor and is assumed to be constant [13, 20] with a value of 5/6. Transformed material constants, for the k^{th} lamina, are denoted by $\overline{Q}_{ij}^{k}$ and are given as follows.

$$\overline{Q}_{11} = Q_{11}\cos^4\theta + 2\left(Q_{12} + 2Q_{66}\right)\sin^2\theta\cos^2\theta + Q_{22}\sin^4\theta \tag{9a}$$

$$\overline{Q}_{12} = \left(Q_{11} + Q_{22} - 4Q_{66}\right)\sin^2\theta\cos^2\theta + Q_{12}\left(\sin^4\theta + \cos^4\theta\right) \tag{9b}$$

$$\overline{Q}_{22} = Q_{11}\sin^4\theta + 2\left(Q_{12} + 2Q_{66}\right)\sin^2\theta\cos^2\theta + Q_{22}\cos^4\theta \tag{9c}$$

$$\overline{Q}_{16} = \left(Q_{11} - Q_{12} - 2Q_{66}\right)\sin\theta\cos^3\theta + \left(Q_{12} - Q_{22} + 2Q_{66}\right)\sin^3\theta\cos\theta \tag{9d}$$

$$\overline{Q}_{26} = \left(Q_{11} - Q_{12} - 2Q_{66}\right)\sin^3\theta\cos\theta + \left(Q_{12} - Q_{22} + 2Q_{66}\right)\sin\theta\cos^3\theta \tag{9e}$$

$$\overline{Q}_{66} = \left(Q_{11} + Q_{22} - 2Q_{12} - 2Q_{66}\right)\sin^2\theta\cos^2\theta + Q_{66}\left(\sin^4\theta + \cos^4\theta\right) \tag{9f}$$

$$\overline{Q}_{55} = G_{13}\cos^2\theta + G_{23}\sin^2\theta \tag{9g}$$

where θ is the fiber angle and Q_{ij} (i, j = 1, 2, 6) in Eq. (9) are given as follows

$$Q_{11} = \frac{E_1}{1-\nu_{12}\nu_{21}} \tag{10a}$$

$$Q_{12} = \frac{\nu_{12}E_2}{1-\nu_{12}\nu_{21}} = \frac{\nu_{21}E_1}{1-\nu_{12}\nu_{21}} \tag{10b}$$

$$Q_{22} = \frac{E_2}{1-\nu_{12}\nu_{21}} \tag{10c}$$

$$Q_{66} = G_{12} \tag{10d}$$

Longitudinal normal stress for generally laminated composite beam can be calculated as follows

$$\sigma_{xx} = \frac{N_x}{h} + 12z\frac{M_x}{h^3} \tag{11}$$

2.4. Hamilton Principle

Hamilton principle is employed for derivation of governing equations and boundary conditions of the problem. It states that

$$\delta\int_{t_1}^{t_2}(K-U+W)dt = 0 \tag{12}$$

where kinetic energy, strain energy and work done by external forces are denoted by *K*, *U* and *W* respectively. Following are the expressions for kinetic energy, strain energy and work done by external forces.

$$U = \frac{1}{2}\int_0^L \left\{N_x\varepsilon_x^0 + M_x\kappa_x + M_{xy}\kappa_{xy} + Q_{xz}\gamma_{xz}\right\}bdx \tag{13}$$

$$K = \frac{1}{2}\int_0^L\int_{-\frac{h}{2}}^{\frac{h}{2}} \rho\left\{\left(\frac{\partial u_x}{\partial t}\right)^2 + \left(\frac{\partial u_y}{\partial t}\right)^2 + \left(\frac{\partial u_z}{\partial t}\right)^2\right\}bdzdx \tag{14}$$

$$W = \int_0^L q(x,t)wdx \tag{15}$$

In order to apply the Hamilton principle, expressions of kinetic and strain energy can be written in displacement form as follows

$$U=\int_0^L\left\{\begin{array}{l}\dfrac{\overline{A}_{11}}{2}u_{,x}^2+\overline{B}_{11}u_{,x}\psi_{x,x}+\overline{B}_{16}u_{,x}\psi_{y,x}+\dfrac{\overline{D}_{11}}{2}\psi_{x,x}^2+\overline{D}_{16}\psi_{y,x}\psi_{x,x}\\+\dfrac{\overline{D}_{66}}{2}\psi_{y,x}^2+\dfrac{\overline{A}_{55}}{2}\left(\psi_x^2+w_{,x}^2+2\psi_x w_{,x}\right)\end{array}\right\}dx \tag{16}$$

$$T=\frac{1}{2}\int_0^L\left\{I_1\left(\dot{u}^2+\dot{w}^2\right)+I_3\left(\dot{\psi}_x^2+\dot{\psi}_y^2\right)+2I_2\dot{u}\dot{\psi}_x\right\}dx \tag{17}$$

where

$$\left(I_1,I_2,I_3\right)=\int_{-\frac{h}{2}}^{\frac{h}{2}}\rho\left(1,z,z^2\right)bdz \tag{18}$$

By substituting Eqs. (15-18) in Eq. (12), we get

$$\delta\int_{t_1}^{t_2}\left[\begin{array}{l}\dfrac{1}{2}\displaystyle\int_0^L\left\{I_1\left(\dot{u}^2+\dot{w}^2\right)+I_3\left(\dot{\psi}_x^2+\dot{\psi}_y^2\right)+2I_2\dot{u}\dot{\psi}_x\right\}dx-\\\displaystyle\int_0^L\left\{\begin{array}{l}\dfrac{\overline{A}_{11}}{2}u_{,x}^2+\overline{B}_{11}u_{,x}\psi_{x,x}+\overline{B}_{16}u_{,x}\psi_{y,x}+\dfrac{\overline{D}_{11}}{2}\psi_{x,x}^2+\overline{D}_{16}\psi_{y,x}\psi_{x,x}\\+\dfrac{\overline{D}_{66}}{2}\psi_{y,x}^2+\dfrac{\overline{A}_{55}}{2}\left(\psi_x^2+w_{,x}^2+2\psi_x w_{,x}\right)\end{array}\right\}dx\\+\displaystyle\int_0^L q\left(x,t\right)wdx\end{array}\right]dt=0 \tag{19}$$

Eq. (19) is cast into the following form after carrying out integration by parts.

$$\int_{t_1}^{t_2}\int_0^L\left[\begin{array}{l}\left\{\begin{array}{l}-I_1\ddot{u}-I_2\ddot{\psi}_x+\overline{A}_{11}u_{,xx}+\overline{B}_{11}\psi_{x,xx}\\+\overline{B}_{16}\psi_{y,xx}\end{array}\right\}\delta u+\\\left\{\begin{array}{l}-I_3\ddot{\psi}_x-I_2\ddot{u}+\overline{D}_{11}\psi_{x,xx}+\overline{B}_{11}u_{,xx}\\+\overline{D}_{16}\psi_{y,xx}-\overline{A}_{55}\left(w_{,x}+\psi_x\right)\end{array}\right\}\delta\psi_x+\\\left\{\begin{array}{l}-I_3\ddot{\psi}_y+\overline{D}_{66}\psi_{y,xx}+\overline{B}_{16}u_{,xx}\\+\overline{D}_{16}\psi_{x,xx}\end{array}\right\}\delta\psi_y+\\\left\{-I_1\ddot{w}+\overline{A}_{55}\left(\psi_{x,x}+w_{,xx}\right)+q\left(x,t\right)\right\}\delta w\end{array}\right]dxdt+\cdots$$

$$
\begin{aligned}
&-\left[\left\{\overline{A}_{11}u_{,x}+\overline{B}_{11}\psi_{x,x}+\overline{B}_{16}\psi_{y,x}\right\}\delta u\right]_0^L\\
&-\left[\left\{\overline{B}_{11}u_{,x}+\overline{D}_{11}\psi_{x,x}+\overline{D}_{16}\psi_{y,x}\right\}\delta\psi_x\right]_0^L\\
&-\left[\left\{\overline{B}_{16}u_{,x}+\overline{D}_{16}\psi_{x,x}+\overline{D}_{66}\psi_{y,x}\right\}\delta\psi_y\right]_0^L\\
&-\left[\left\{\overline{A}_{55}\left(\psi_x+w_{,x}\right)\right\}\delta w\right]_0^L
\end{aligned}
= 0 \qquad (20)
$$

Following are the equations of motion obtained from Eq. (20).

$$\overline{A}_{11}u_{,xx}+\overline{B}_{11}\psi_{x,xx}+\overline{B}_{16}\psi_{y,xx}=I_1\ddot{u}+I_2\ddot{\psi}_x \qquad (21a)$$

$$\overline{D}_{11}\psi_{x,xx}+\overline{B}_{11}u_{,xx}+\overline{D}_{16}\psi_{y,xx}-\overline{A}_{55}\left(w_{,x}+\psi_x\right)=I_3\ddot{\psi}_x+I_2\ddot{u} \qquad (21b)$$

$$\overline{D}_{66}\psi_{y,xx}+\overline{B}_{16}u_{,xx}+\overline{D}_{16}\psi_{x,xx}=I_3\ddot{\psi}_y \qquad (21c)$$

$$\overline{A}_{55}\left(\psi_{x,x}+w_{,xx}\right)+q(x,t)=I_1\ddot{w} \qquad (21d)$$

By using Eqs. (4) and (5), natural and essential boundary conditions obtained from Eq. (20) are given below.

$$u=0 \quad \text{or} \quad N_x=0 \qquad (22a)$$

$$\psi_x=0 \ \text{or} \ M_x=0 \qquad (22b)$$

$$\psi_y=0 \ \text{or} \ M_{xy}=0 \qquad (22c)$$

$$w=0 \quad \text{or} \ Q_{xz}=0 \qquad (22d)$$

CHAPTER 3

D-BEM FORMULATION

In Boundary Element Method, fundamental solution of differential operator is employed as weight function in weighted residual statement. Fundamental solutions, employed here, are independent of time and are found using reduced non-homogeneous forms of differential equations. Time derivative and coupled quantities in the differential equations are discarded while deriving the static fundamental solution. The steady-state nature of fundamental solutions eventuates in Domain-Boundary element method.

3.1. Fundamental Solutions

In case of ordinary differential equation of n^{th} order, having constant coefficients, fundamental solution satisfies the following relation

$$\boldsymbol{L}\left[v^*\left(x,\xi\right)\right]=\delta\left(x-\xi\right) \tag{23}$$

where $\delta\left(x-\xi\right)$ is Dirac delta function and differential operator $\boldsymbol{L}$ is given by

$$\boldsymbol{L}=\frac{d^n}{dx^n}+a_1\frac{d^{n-1}}{dx^{n-1}}+a_2\frac{d^{n-2}}{dx^{n-2}}+\cdots\cdots\cdots\cdots+a_{n-1}\frac{d}{dx}+a_n \tag{24}$$

In Eq. (23), $v^*\left(x,\xi\right)$ is fundamental solution and is given as follows

$$v^*\left(x,\xi\right)=H\left(x-\xi\right)v\left(x,\xi\right) \tag{25}$$

where $H\left(x-\xi\right)$ is the Heaviside unit step function and it is related to Dirac delta as follows

$$\frac{d}{dx}\left[H\left(x-\xi\right)\right]=\delta\left(x-\xi\right) \tag{26}$$

First derivative of fundamental solution, mentioned in Eq. (25) is given as

$$\frac{dv^*}{dx} = \delta(x-\xi)v(x,\xi) + H(x-\xi)v'(x,\xi) \tag{27}$$

Let $v(x,\xi) = 0$ at $x = \xi$

$$\Rightarrow \frac{dv^*}{dx} = H(x-\xi)v'(x,\xi) \tag{28}$$

By taking derivative of Eq. (28), we have

$$\frac{d^2v^*}{dx^2} = \delta(x-\xi)v'(x,\xi) + H(x-\xi)v''(x,\xi) \tag{29}$$

Let $v'(x,\xi) = 0$ at $x = \xi$

$$\Rightarrow \frac{d^2v^*}{dx^2} = H(x-\xi)v''(x,\xi) \tag{30}$$

Similarly, let $v^{n-2}(x,\xi) = 0$ at $x = \xi$, where "*n-2"* is the order of the derivative.

$$\Rightarrow \frac{d^{n-1}v^*}{dx^{n-1}} = H(x-\xi)v^{n-1}(x,\xi) \tag{31}$$

By differentiating Eq. (31) with respect to *x* we get

$$\frac{d^nv^*}{dx^n} = \delta(x-\xi)v^{n-1}(x,\xi) + H(x-\xi)v^n(x,\xi) \tag{32}$$

Let $v^{n-1}(x,\xi) = 1$ at $x = \xi$

$$\frac{d^nv^*}{dx^n} = \delta(x-\xi) + H(x-\xi)v^n(x,\xi) \tag{33}$$

By expanding Eq. (23) and using Eqs. (24) to (33), following equations are obtained.

$$\begin{aligned}&\delta(x-\delta) + H(x-\xi)v^n(x,\xi) + a_1H(x-\xi)v^{n-1}(x,\xi) + \cdots \\ &\cdots + a_{n-1}H(x-\xi)v'(x,\xi) + a_nH(x-\xi)v(x,\xi) = \delta(x-\delta)\end{aligned} \tag{34}$$

$$\Rightarrow H(x-\xi)\boldsymbol{L}\left[v(x,\xi)\right] = 0 \tag{35}$$

$$\Rightarrow \boldsymbol{L}\left[v(x,\xi)\right] = 0 \tag{36}$$

Hence fundamental solution is given by

$$v^*(x,\xi) = H(x-\xi)v(x,\xi) \tag{37}$$

where

$$\boldsymbol{L}\left[v(x,\xi)\right] = 0 \tag{38}$$

and for a differential operator of n^{th} order, we have

$$\begin{aligned} &v(x=\xi) = v'(x=\xi) = v''(x=\xi) = \cdots\cdots = v^{n-2}(x=\xi) = 0 \\ &v^{n-1}(x=\xi) = 1 \end{aligned} \tag{39}$$

3.1.1. Fundamental Solution of Equation 1

Following inhomogeneous form is used for finding the fundamental solution of Eq. (21a):

$$\frac{d^2u^*(x,\xi)}{dx^2} = \delta(x-\xi) \tag{40}$$

In Eq. (40) $u^*(x,\xi)$ is the fundamental solution. ξ represents the source point, x represents the field point and $\delta(x-\xi)$ represents the Dirac delta function. We have

$$u^*(x,\xi) = H(x-\xi)u(x,\xi) \tag{41}$$

Following relation is obtained by differentiating Eq. (41) twice and using Eq. (39).

$$\Rightarrow \frac{d^2u^*(x,\xi)}{dx^2} = H(x-\xi)\frac{d^2u(x,\xi)}{dx^2} + \delta(x-\xi) \tag{42}$$

Substitution of Eq. (42) in Eq. (40) results in

$$H(x-\xi)\frac{d^2u(x,\xi)}{dx^2} + \delta(x-\xi) = \delta(x-\xi) \tag{43a}$$

$$\Rightarrow H(x-\xi)\frac{d^2u(x,\xi)}{dx^2} = 0 \tag{43b}$$

$$\Rightarrow \frac{d^2u(x,\xi)}{dx^2} = 0 \tag{43c}$$

After integrating Eq. (43c) twice, we get

$$u(x,\xi) = C_1 x + C_2 \tag{44}$$

Let $u(x,\xi) = 0$ at $x = \xi$ & $u'(x,\xi) = 1$ at $x = \xi$. By applying these conditions, C_1 and C_2 are found and Eq. (44) can be written as follows

$$u(x,\xi) = (x - \xi) \tag{45}$$

$$\Rightarrow u^*(x,\xi) = (x - \xi) H(x - \xi) \tag{46}$$

Any constant multiple of a solution and addition of two solutions is also a solution so

$$u^*(x,\xi) = (x - \xi) H(x - \xi) - \frac{1}{2}(x - \xi) \tag{47a}$$

$$\Rightarrow u^*(x,\xi) = \frac{(x - \xi)}{2}\{2H(x - \xi) - 1\} \tag{47b}$$

$$\Rightarrow u^*(x,\xi) = \frac{|x - \xi|}{2} \tag{47c}$$

3.1.2. Fundamental Solution of Equation 2

In order to find the fundamental solution of Eq. (21b), following inhomogeneous form is used.

$$\frac{d^2\psi_x^*(x,\xi)}{dx^2} - \frac{\overline{A}_{55}}{\overline{D}_{11}}\psi_x^*(x,\xi) = \delta(x - \xi) \tag{48}$$

Let $\frac{\overline{A}_{55}}{\overline{D}_{11}} = \lambda$

$$\frac{d^2\psi_x^*(x,\xi)}{dx^2} - \lambda\psi_x^*(x,\xi) = \delta(x - \xi) \tag{49}$$

In Eq. (49) $\psi_x^*(x,\xi)$ is the fundamental solution. ξ represents the source point, x represents the field point and $\delta(x - \xi)$ represents the Dirac delta function. We have

$$\psi_x^*(x,\xi) = H(x - \xi)\psi_x(x,\xi) \tag{50}$$

By differentiating Eq. (50) two times with respect to *x* and using Eq. (39) results in

$$\Rightarrow \frac{d^2\psi_x^*(x,\xi)}{dx^2} = H(x-\xi)\frac{d^2\psi_x(x,\xi)}{dx^2} + \delta(x-\xi) \tag{51}$$

Substitution of Eqs. (50) & (51) in Eq. (49) gives

$$H(x-\xi)\frac{d^2\psi_x(x,\xi)}{dx^2} + \delta(x-\xi) - \lambda H(x-\xi)\psi_x(x,\xi) = \delta(x-\xi) \tag{52a}$$

$$\Rightarrow H(x-\xi)\left\{\frac{d^2\psi_x(x,\xi)}{dx^2} - \lambda\psi_x(x,\xi)\right\} = 0 \tag{52b}$$

$$\Rightarrow \frac{d^2\psi_x(x,\xi)}{dx^2} - \lambda\psi_x(x,\xi) = 0 \tag{52c}$$

Let $\psi_x = e^{rx}$. Eq. (52c) implies

$$r^2e^{rx} - \lambda e^{rx} = 0 \Rightarrow r = \pm\sqrt{\lambda} \tag{53}$$

Solution to eq. (52c) can be written as

$$\psi_x(x,\xi) = \mathrm{C}_1e^{\sqrt{\lambda}x} + \mathrm{C}_2e^{-\sqrt{\lambda}x} \tag{54}$$

Let $\psi_x(x,\xi) = 0$ at $x = \xi$ & $\psi_x'(x,\xi) = 1$ at $x = \xi$, we have

$$\mathrm{C}_1e^{\sqrt{\lambda}\xi} + \mathrm{C}_2e^{-\sqrt{\lambda}\xi} = 0 \tag{55a}$$

$$\mathrm{C}_1\sqrt{\lambda}e^{\sqrt{\lambda}\xi} + \mathrm{C}_2\sqrt{\lambda}e^{-\sqrt{\lambda}\xi} = 1 \tag{55b}$$

C_1 & C_2 are obtained as follows after the solution of Eq. (55a) and Eq. (55b)

$$\mathrm{C}_1 = \frac{1}{2\sqrt{\lambda}e^{\sqrt{\lambda}\xi}} \tag{56a}$$

$$\mathrm{C}_2 = \frac{-1}{2\sqrt{\lambda}e^{-\sqrt{\lambda}\xi}} \tag{56b}$$

Eq. (54) can be written as

$$\psi_x = \frac{1}{2\sqrt{\lambda}}\left\{e^{\sqrt{\lambda}(x-\xi)} - e^{-\sqrt{\lambda}(x-\xi)}\right\} \tag{57}$$

By substituting Eq. (57) in Eq. (50), we get

$$\psi_x^*(x,\xi)=\frac{1}{2\sqrt{\lambda}}\left\{e^{\sqrt{\lambda}(x-\xi)}-e^{-\sqrt{\lambda}(x-\xi)}\right\}H(x-\xi) \tag{58}$$

Any constant multiple of a solution and addition of two solutions is also a solution so

$$\psi_x^*(x,\xi)=\frac{1}{2\sqrt{\lambda}}\left\{e^{\sqrt{\lambda}(x-\xi)}-e^{-\sqrt{\lambda}(x-\xi)}\right\}H(x-\xi)-\frac{1}{4\sqrt{\lambda}}\left\{e^{\sqrt{\lambda}(x-\xi)}-e^{-\sqrt{\lambda}(x-\xi)}\right\} \tag{59a}$$

$$\Rightarrow\psi_x^*(x,\xi)=\frac{1}{2\sqrt{\lambda}}\left\{\frac{e^{\sqrt{\lambda}(x-\xi)}-e^{-\sqrt{\lambda}(x-\xi)}}{2}\right\}\left\{2H(x-\xi)-1\right\} \tag{59b}$$

$$\Rightarrow\psi_x^*(x,\xi)=\frac{1}{2\sqrt{\lambda}}\sinh\left[\sqrt{\lambda}(x-\xi)\right]\left\{2H(x-\xi)-1\right\} \tag{59c}$$

$$\Rightarrow\psi_x^*(x,\xi)=\frac{1}{2\sqrt{\lambda}}\sinh\left[\sqrt{\lambda}\,|\,x-\xi\,|\right] \tag{59d}$$

3.1.3. Fundamental Solution of Equation 3

Eq. (60) is the non-homogeneous form utilized in calculating the fundamental solution of Eq. (21c):

$$\frac{d^2\psi_y^*(x,\xi)}{dx^2}=\delta(x-\xi) \tag{60}$$

$\psi_y^*(x,\xi)$ is the fundamental solution. ξ represents the source point, *x* represents the field point and $\delta(x-\xi)$ represents the Dirac delta function. We have

$$\psi_y^*(x,\xi)=H(x-\xi)\psi_y(x,\xi) \tag{61}$$

Differentiating the above equation twice with respect to *x* and using Eq. (39) results in

$$\Rightarrow\frac{d^2\psi_y^*(x,\xi)}{dx^2}=H(x-\xi)\frac{d^2\psi_y(x,\xi)}{dx^2}+\delta(x-\xi) \tag{62}$$

By substituting Eq. (62) in Eq. (60) we get

$$H(x-\xi)\frac{d^2\psi_y(x,\xi)}{dx^2}+\delta(x-\xi)=\delta(x-\xi) \tag{63a}$$

$$\Rightarrow H(x-\xi)\frac{d^2\psi_y(x,\xi)}{dx^2}=0 \tag{63b}$$

$$\Rightarrow \frac{d^2\psi_y(x,\xi)}{dx^2}=0 \tag{63c}$$

Integrating Eq. (63c) twice, results in

$$\psi_y(x,\xi)=C_1x+C_2 \tag{64}$$

Let $\psi_y(x,\xi)=0$ at $x=\xi$ & $\psi_y'(x,\xi)=1$ at $x=\xi$. Solution of Eq. (64) for C_1 and C_2, gives the following

$$\psi_y(x,\xi)=(x-\xi) \tag{65}$$

$$\Rightarrow \psi_y^*(x,\xi)=(x-\xi)H(x-\xi) \tag{66}$$

Any constant multiple of a solution and addition of two solutions is also a solution so

$$\psi_y^*(x,\xi)=(x-\xi)H(x-\xi)-\frac{1}{2}(x-\xi) \tag{67a}$$

$$\Rightarrow \psi_y^*(x,\xi)=\frac{(x-\xi)}{2}\{2H(x-\xi)-1\} \tag{67b}$$

$$\Rightarrow \psi_y^*(x,\xi)=\frac{|x-\xi|}{2} \tag{67c}$$

3.1.4. Fundamental Solution of Equation 4

Eq. (68) shows the non-homogeneous form used for finding the fundamental solution of Eq. (21d):

$$\frac{d^2w^*(x,\xi)}{dx^2}=\delta(x-\xi) \tag{68}$$

$w^*(x,\xi)$ is the fundamental solution. ξ represents the source point, *x* represents the field point and $\delta(x-\xi)$ represents the Dirac delta function. We have

$$w^*(x,\xi) = H(x-\xi)\,w(x,\xi) \tag{69}$$

By differentiating Eq. (69) twice and using Eq. (39), following equation is obtained

$$\Rightarrow \frac{d^2 w^*(x,\xi)}{dx^2} = H(x-\xi)\frac{d^2 w(x,\xi)}{dx^2} + \delta(x-\xi) \tag{70}$$

Substitution of Eq. (70) in Eq. (68) gives the following

$$H(x-\xi)\frac{d^2 w(x,\xi)}{dx^2} + \delta(x-\xi) = \delta(x-\xi) \tag{71a}$$

$$\Rightarrow H(x-\xi)\frac{d^2 w(x,\xi)}{dx^2} = 0 \tag{71b}$$

$$\Rightarrow \frac{d^2 w(x,\xi)}{dx^2} = 0 \tag{71c}$$

After integrating Eq. (71c) twice, we get

$$w(x,\xi) = \mathrm{C}_1 x + \mathrm{C}_2 \tag{72}$$

Let $w(x,\xi) = 0$ at $x = \xi$ & $w'(x,\xi) = 1$ at $x = \xi$. Solving for C_1 and C_2 results in

$$w^*(x,\xi) = (x-\xi) \tag{73}$$

$$w^*(x,\xi) = (x-\xi)H(x-\xi) \tag{74}$$

Any constant multiple of a solution and addition of two solutions is also a solution so

$$w^*(x,\xi) = (x-\xi)H(x-\xi) - \frac{1}{2}(x-\xi) \tag{75a}$$

$$\Rightarrow w^*(x,\xi) = \frac{(x-\xi)}{2}\{2H(x-\xi)-1\} \tag{75b}$$

$$\Rightarrow w^*(x,\xi) = \frac{|x-\xi|}{2} \tag{75c}$$

3.2. Weighted Residual Statement

Equations of motion of generally laminated composite beam are written as follows in the weighted residual statement:

$$\int_0^L \left\{ \overline{A}_{11} u_{,xx} + \overline{B}_{11} \psi_{x,xx} + \overline{B}_{16} \psi_{y,xx} - I_1 \ddot{u} - I_2 \ddot{\psi}_x \right\} u^*(x,\xi)\, dx = 0 \tag{76a}$$

$$\int_0^L \left\{ \overline{D}_{11} \psi_{x,xx} + \overline{B}_{11} u_{,xx} + \overline{D}_{16} \psi_{y,xx} - \overline{A}_{55} \left(w_{,x} + \psi_x \right) - I_3 \ddot{\psi}_x - I_2 \ddot{u} \right\} \psi_x^*(x,\xi)\, dx = 0 \tag{76b}$$

$$\int_0^L \left\{ \overline{D}_{66} \psi_{y,xx} + \overline{B}_{16} u_{,xx} + \overline{D}_{16} \psi_{x,xx} - I_3 \ddot{\psi}_y \right\} \psi_y^*(x,\xi)\, dx = 0 \tag{76c}$$

$$\int_0^L \left\{ \overline{A}_{55} \left(\psi_{x,x} + w_{,xx} \right) + q(x,t) - I_1 \ddot{w} \right\} w^*(x,\xi)\, dx = 0 \tag{76d}$$

Application of integration by parts results in the following form of Eq. (76)

$$\begin{aligned}
&\int_0^L \overline{A}_{11} u(x,t) u^*_{,xx}(x,\xi)\, dx = -\int_0^L \left\{ \overline{B}_{16} \psi_y(x,t) + \overline{B}_{11} \psi_x(x,t) \right\} (u^*_{,xx}(x,\xi))\, dx \\
&- \left[\left\{ \overline{A}_{11} u_{,x}(x,t) + \overline{B}_{16} \psi_{y,x}(x,t) + \overline{B}_{11} \psi_{x,x}(x,t) \right\} u^*(x,\xi) \right]_0^L \\
&+ \left[\left\{ \overline{A}_{11} u(x,t) + \overline{B}_{16} \psi_y(x,t) + \overline{B}_{11} \psi_x(x,t) \right\} \left(u^*_{,x}(x,\xi) \right) \right]_0^L \\
&+ \int_0^L \left\{ I_1 \ddot{u}(x,t) + I_2 \ddot{\psi}_x(x,t) \right\} u^*(x,\xi) dx
\end{aligned} \tag{77a}$$

$$\begin{aligned}
&\int_0^L \overline{D}_{11} \psi_x(x,t) \left\{ \psi^*_{x,xx}(x,\xi) - \frac{\overline{A}_{55}}{\overline{D}_{11}} \psi^*_x(x,\xi) \right\} dx = \\
&- \left[\left\{ \overline{B}_{11} u_{,x}(x,t) + \overline{D}_{11} \psi_{x,x}(x,t) + \overline{D}_{16} \psi_{y,x}(x,t) \right\} \psi^*_x(x,\xi) \right]_0^L \\
&+ \left[\left\{ \overline{D}_{11} \psi_x(x,t) + \overline{B}_{11} u(x,t) + \overline{D}_{16} \psi_y(x,t) \right\} \left(\psi^*_{x,x}(x,\xi) \right) \right]_0^L \\
&- \overline{A}_{55} \left[w(x,t) \psi^*_x(x,\xi) \right]_0^L - \int_0^L \left\{ \overline{B}_{11} u(x,t) + \overline{D}_{16} \psi_y(x,t) \right\} \left(\psi^*_{x,xx}(x,\xi) \right) dx
\end{aligned} \tag{77b}$$

$$+\int_0^L \left\{ I_2 \ddot{u}(x,t) + I_3 \ddot{\psi}_x(x,t) \right\} dx + \int_0^L \overline{A}_{55} w(x,t) \psi^*_{x,x}(x,\xi) dx$$

$$\int_0^L \overline{D}_{66} \psi_y(x,t) \psi^*_{y,xx}(x,\xi) dx = \int_0^L I_3 \ddot{\psi}_y(x,t) \psi^*_y(x,\xi) dx$$
$$-\left[\left\{ \overline{B}_{16} u_{,x}(x,t) + \overline{D}_{66} \psi_{y,x}(x,t) + \overline{D}_{16} \psi_{x,x}(x,t) \right\} \psi^*_y(x,\xi) \right]_0^L$$
$$+\left[\left\{ \overline{D}_{66} \psi_y(x,t) + \overline{B}_{16} u(x,t) + \overline{D}_{16} \psi_x(x,t) \right\} \left(\psi^*_{y,x}(x,\xi) \right) \right]_0^L \quad (77c)$$
$$-\int_0^L \left\{ \overline{B}_{16} u(x,t) + \overline{D}_{16} \psi_x(x,t) \right\} \left(\psi^*_{y,xx}(x,\xi) \right) dx$$

$$\int_0^L \overline{A}_{55} w(x,t) w^*_{,xx}(x,\xi) dx = \overline{A}_{55} \left[w(x,t) w^*_{,x}(x,\xi) \right]_0^L$$
$$-\left[\overline{A}_{55} \left\{ \psi_x(x,t) + w_{,x}(x,t) \right\} w^*(x,\xi) \right]_0^L \quad (77d)$$
$$+\int_0^L \overline{A}_{55} \psi_x(x,t) w^*_{,x}(x,\xi) dx - \int_0^L \left\{ q(x,t) - I_1 \ddot{w}(x,t) \right\} w^*(x,\xi) dx$$

By using Eqs. (2b), (3), (4) and (5), following form of Eq. (77) is obtained:

$$\int_0^L \overline{A}_{11} u(x,t) u^*_{,xx}(x,\xi) dx = -\left[N_x(x,t) u^*(x,\xi) \right]_0^L$$
$$-\int_0^L \left\{ \overline{B}_{16} \psi_y(x,t) + \overline{B}_{11} \psi_x(x,t) \right\} (u^*_{,xx}(x,\xi)) dx$$
$$+\left[\left\{ \overline{A}_{11} u(x,t) + \overline{B}_{16} \psi_y(x,t) + \overline{B}_{11} \psi_x(x,t) \right\} \left(u^*_{,x}(x,\xi) \right) \right]_0^L \quad (78a)$$
$$+\int_0^L \left\{ I_1 \ddot{u}(x,t) + I_2 \ddot{\psi}_x(x,t) \right\} u^*(x,\xi) dx$$

$$\int_0^L \overline{D}_{11} \psi_x(x,t) \left\{ \psi^*_{x,xx}(x,\xi) - \frac{\overline{A}_{55}}{\overline{D}_{11}} \psi^*_x(x,\xi) \right\} dx = -\left[M_x(x,t) \psi^*_x(x,\xi) \right]_0^L \quad (78b)$$
$$+\left[\left\{ \overline{D}_{11} \psi_x(x,t) + \overline{B}_{11} u(x,t) + \overline{D}_{16} \psi_y(x,t) \right\} \left(\psi^*_{x,x}(x,\xi) \right) \right]_0^L$$

$$-\overline{A}_{55}\left[w(x,t)\psi_x^*(x,\xi)\right]_0^L-\int_0^L\left\{\overline{B}_{11}u(x,t)+\overline{D}_{16}\psi_y(x,t)\right\}\left(\psi_{x,xx}^*(x,\xi)\right)dx$$
$$+\int_0^L\left\{I_2\ddot{u}(x,t)+I_3\ddot{\psi}_x(x,t)\right\}dx+\int_0^L\overline{A}_{55}w(x,t)\psi_{x,x}^*(x,\xi)dx$$

$$\int_0^L\overline{D}_{66}\psi_y(x,t)\psi_{y,xx}^*(x,\xi)dx=-\left[M_{xy}(x,t)\psi_y^*(x,\xi)\right]_0^L+\int_0^L I_3\ddot{\psi}_y(x,t)\psi_y^*(x,\xi)dx$$
$$+\left[\left\{\overline{D}_{66}\psi_y(x,t)+\overline{B}_{16}u(x,t)+\overline{D}_{16}\psi_x(x,t)\right\}\left(\psi_{y,x}^*(x,\xi)\right)\right]_0^L \tag{78c}$$
$$-\int_0^L\left\{\overline{B}_{16}u(x,t)+\overline{D}_{16}\psi_x(x,t)\right\}\left(\psi_{y,xx}^*(x,\xi)\right)dx$$

$$\int_0^L\overline{A}_{55}w(x,t)w_{,xx}^*(x,\xi)dx=-\left[Q_{xz}(x,t)w^*(x,\xi)\right]_0^L+\overline{A}_{55}\left[w(x,t)w_{,x}^*(x,\xi)\right]_0^L$$
$$+\int_0^L\overline{A}_{55}\psi_x(x,t)w_{,x}^*(x,\xi)dx-\int_0^L\left\{q(x,t)-I_1\ddot{w}(x,t)\right\}w^*(x,\xi)dx \tag{78d}$$

After using Eqs. (40), (49), (60) and (68), governing integral equations of the problem are written in the following form:

$$u(\xi,t)+\frac{\overline{B}_{11}}{\overline{A}_{11}}\psi_x(\xi,t)+\frac{\overline{B}_{16}}{\overline{A}_{11}}\psi_y(\xi,t)=-\left[N_x(x,t)u^*(x,\xi)\right]_0^L$$
$$+\left[\left\{\overline{A}_{11}u(x,t)+\overline{B}_{11}\psi_x(x,t)+\overline{B}_{16}\psi_y(x,t)\right\}\left(u_{,x}^*(x,\xi)\right)\right]_0^L \tag{79a}$$
$$+\int_0^L\left\{I_1\ddot{u}(x,t)+I_2\ddot{\psi}_x(x,t)\right\}(u^*(x,\xi))dx$$

$$\psi_x(\xi,t)+\frac{\overline{B}_{11}}{\overline{D}_{11}}u(\xi,t)+\frac{\overline{D}_{16}}{\overline{D}_{11}}\psi_y(\xi,t)=-\left[M_x(x,t)\psi_x^*(\xi,t)\right]_0^L$$
$$+\left[\left\{\overline{D}_{11}\psi_x(x,t)+\overline{B}_{11}u(x,t)+\overline{D}_{16}\psi_y(x,t)\right\}\left(\psi_{x,x}^*(x,\xi)\right)\right]_0^L \tag{79b}$$
$$-\overline{A}_{55}\left[w(x,t)\psi_x^*(x,\xi)\right]_0^L-\int_0^L\lambda\left\{\overline{B}_{11}u(x,t)+\overline{D}_{16}\psi_y(x,t)\right\}(\psi_x^*(x,\xi))dx$$

$$+\int_0^L \overline{A}_{55} w(x,t)\psi^*_{x,x}(x,\xi)dx + \int_0^L \left\{ I_2 \ddot{u}(x,t) + I_3 \ddot{\psi}_x(x,t) \right\} \left(\psi^*_x(x,\xi) \right) dx$$

$$\psi_y(\xi,t) + \frac{\overline{B}_{16}}{\overline{D}_{66}} u(\xi,t) + \frac{\overline{D}_{16}}{\overline{D}_{66}} \psi_x(\xi,t) = -\left[M_{xy}(x,t)\psi^*_y(x,\xi) \right]_0^L$$

$$+\left[\left\{ \overline{D}_{66}\psi_y(x,t) + \overline{B}_{16}u(x,t) + \overline{D}_{16}\psi_x(x,t) \right\} \left(\psi^*_{y,x}(x,\xi) \right) \right]_0^L \qquad (79c)$$

$$+\int_0^L I_3 \ddot{\psi}_y(x,t)\psi^*_y(x,\xi)dx$$

$$w(\xi,t) = -\left[Q_{xz}(x,t)w^*(x,\xi) \right]_0^L + \overline{A}_{55} \left[w(x,t)w^*_{,x}(x,\xi) \right]_0^L$$

$$+\int_0^L \overline{A}_{55}\psi_x(x,t)w^*_{,x}(x,\xi)dx - \int_0^L \left\{ q(x,t) - I_1 \ddot{w}(x,t) \right\} w^*(x,\xi)dx \qquad (79d)$$

In order to evaluate the domain integrals in Eq. (79), whole domain is divided into quadratic cells as shown in Fig. 4. Each cell has three nodes and number of nodes N is related to number of cells via $M = (N-1)/2$. In j^{th} cell, $\Omega_j = \left[x_1^j, x_3^j \right]$, $1 \le j \le M$; first, middle and last coordinate of j^{th} cell are represented by x_1^j, x_2^j and x_3^j respectively.

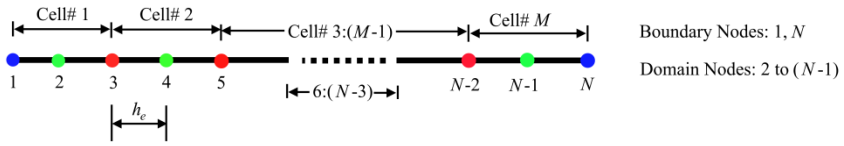

Figure 4: Discretization of domain

In order to approximate the value of a generic field variable $\Theta\left(x_i^j, t\right)$, at node *'i'* and time *'t'* in j^{th} cell, following equation is employed.

$$\Theta = \phi_1^j(x)\Theta(x_1^j,t) + \phi_2^j(x)\Theta(x_2^j,t) + \phi_3^j(x)\Theta(x_3^j,t) \qquad (80)$$

where $\phi_i^j(x)$ are polynomial interpolation functions of second degree and are given as follows

$$\phi_1^j(x)=\frac{\left(x-x_2^j\right)\left(x-x_3^j\right)}{2h_e^2} \tag{81a}$$

$$\phi_2^j(x)=-\frac{\left(x-x_1^j\right)\left(x-x_3^j\right)}{h_e^2} \tag{81b}$$

$$\phi_3^j(x)=\frac{\left(x-x_1^j\right)\left(x-x_2^j\right)}{2h_e^2} \tag{81c}$$

and $h_e=x_2^j-x_1^j=x_3^j-x_2^j$ is equal to half length of a cell.

Domain integral involving the load term, in Eq. (79d), will be evaluated depending on type of the applied force. Governing equations in final form, after employing domain discretization, are given in Eq. (82):

$$\begin{aligned}
&u(\xi,t)+\frac{\overline{B}_{11}}{\overline{A}_{11}}\psi_x(\xi,t)+\frac{\overline{B}_{16}}{\overline{A}_{11}}\psi_y(\xi,t)-\frac{1}{2}\left[u\left(0,t\right)+u\left(0,t\right)\right]\\
&-\frac{\overline{B}_{11}}{2\overline{A}_{11}}\left[\psi_x\left(0,t\right)+\psi_x\left(0,t\right)\right]-\frac{\overline{B}_{16}}{2\overline{A}_{11}}\left[\psi_y(0,t)+\psi_y(L,t)\right]\\
&=\frac{1}{2\overline{A}_{11}}\left[N_x(0,t)\left(\xi\right)-N_x(L,t)\left(L-\xi\right)\right]\\
&+\sum_{j=1}^{M}\int_{x_1^j}^{x_3^j}u^*\left(x,\xi\right)\begin{Bmatrix}\phi_1^j\left(x\right)\left[I_1\ddot{u}\left(x_1^j,t\right)+I_2\ddot{\psi}_x\left(x_1^j,t\right)\right]\\+\phi_2^j\left(x\right)\left[I_1\ddot{u}\left(x_2^j,t\right)+I_2\ddot{\psi}_x\left(x_2^j,t\right)\right]\\+\phi_3^j\left(x\right)\left[I_1\ddot{u}\left(x_3^j,t\right)+I_2\ddot{\psi}_x\left(x_3^j,t\right)\right]\end{Bmatrix}dx
\end{aligned} \tag{82a}$$

$$\begin{aligned}
&\psi_y\left(\xi,t\right)+\frac{\overline{B}_{16}}{\overline{D}_{66}}u\left(\xi,t\right)+\frac{\overline{D}_{16}}{\overline{D}_{66}}\psi_x\left(\xi,t\right)-\frac{1}{2}\left[\psi_y\left(0,t\right)+\psi_y\left(L,t\right)\right]\\
&-\frac{\overline{B}_{16}}{2\overline{D}_{66}}\left[u\left(0,t\right)+u\left(L,t\right)\right]-\frac{\overline{D}_{16}}{2\overline{D}_{66}}\left[\psi_x\left(0,t\right)+\psi_x\left(L,t\right)\right]\\
&=\frac{1}{2\overline{D}_{66}}\left[M_{xy}\left(0,t\right)\left(\xi\right)-M_{xy}\left(L,t\right)\left(L-\xi\right)\right]
\end{aligned} \tag{82b}$$

$$+\sum_{j=1}^{M}\int_{x_1^j}^{x_3^j} I_3\psi_y^*(x,\xi)\left\{\phi_1^j(x)\ddot{\psi}_y\left(x_1^j,t\right)+\phi_2^j(x)\ddot{\psi}_y\left(x_2^j,t\right)+\phi_3^j(x)\ddot{\psi}_y\left(x_3^j,t\right)\right\}dx$$

$$w(\xi,t)-\frac{1}{2}\left[w(0,t)+w(0,t)\right]$$

$$-\sum_{j=1}^{M}\int_{x_1^j}^{x_3^j}\overline{A}_{55}w_{,x}^*(x,\xi)\left\{\phi_1^j(x)\psi_x\left(x_1^j,t\right)+\phi_2^j(x)\psi_x\left(x_2^j,t\right)+\phi_3^j(x)\psi_x\left(x_3^j,t\right)\right\}dx$$
$$=\frac{1}{2\overline{A}_{55}}\left[Q_{xz}(0,t)(\xi)-Q_{xz}(L,t)(L-\xi)\right]-\int_0^L q(x,t)w^*(x,\xi)dx \quad (82c)$$
$$+\sum_{j=1}^{M}\int_{x_1^j}^{x_3^j} I_1w^*(x,\xi)\left\{\phi_1^j(x)\ddot{w}\left(x_1^j,t\right)+\phi_2^j(x)\ddot{w}\left(x_2^j,t\right)+\phi_3^j(x)\ddot{w}\left(x_3^j,t\right)\right\}dx$$

$$\psi_x(\xi,t)+\frac{\overline{B}_{11}}{\overline{D}_{11}}u(\xi,t)+\frac{\overline{D}_{16}}{\overline{D}_{11}}\psi_y(\xi,t)$$

$$-\frac{1}{2}\left\{\psi_x(0,t)\cosh\left[\sqrt{\lambda}(\xi)\right]+\psi_x(L,t)\cosh\left[\sqrt{\lambda}(L-\xi)\right]\right\}$$
$$-\frac{\overline{B}_{11}}{2\overline{D}_{11}}\left\{u(0,t)\cosh\left[\sqrt{\lambda}(\xi)\right]+u(L,t)\cosh\left[\sqrt{\lambda}(L-\xi)\right]\right\}$$
$$-\frac{\overline{D}_{16}}{2\overline{D}_{11}}\left\{\psi_y(0,t)\cosh\left[\sqrt{\lambda}(\xi)\right]+\psi_y(L,t)\cosh\left[\sqrt{\lambda}(L-\xi)\right]\right\}$$
$$+\frac{\overline{A}_{55}}{2\overline{D}_{11}\sqrt{\lambda}}\left\{w(0,t)\sinh\left[\sqrt{\lambda}(\xi)\right]-w(L,t)\sinh\left[\sqrt{\lambda}(L-\xi)\right]\right\} \quad (82d)$$
$$+\sum_{j=1}^{M}\int_{x_1^j}^{x_3^j}\lambda\overline{B}_{11}\psi_x^*(x,\xi)\left\{\phi_1^j(x)u\left(x_1^j,t\right)+\phi_2^j(x)u\left(x_2^j,t\right)+\phi_3^j(x)u\left(x_3^j,t\right)\right\}dx$$
$$+\sum_{j=1}^{M}\int_{x_1^j}^{x_3^j}\lambda\overline{D}_{16}\psi_x^*(x,\xi)\begin{Bmatrix}\phi_1^j(x)\psi_y\left(x_1^j,t\right)+\phi_2^j(x)\psi_y\left(x_2^j,t\right)\\+\phi_3^j(x)\psi_y\left(x_3^j,t\right)\end{Bmatrix}dx$$
$$+\sum_{j=1}^{M}\int_{x_1^j}^{x_3^j}\overline{A}_{55}\psi_{x,x}^*(x,\xi)\left\{\phi_1^j(x)w\left(x_1^j,t\right)+\phi_2^j(x)w\left(x_2^j,t\right)+\phi_3^j(x)w\left(x_3^j,t\right)\right\}dx$$
$$=\frac{1}{2\overline{D}_{11}\sqrt{\lambda}}\left\{M_x(0,t)\sinh\left[\sqrt{\lambda}(\xi)\right]-M_x(L,t)\sinh\left[\sqrt{\lambda}(L-\xi)\right]\right\}$$

$$+\sum_{j=1}^{M}\int_{x_1^j}^{x_3^j}\psi_x^*\left(x,\xi\right)\begin{Bmatrix}\phi_1^j\left(x\right)\left[I_2\ddot{u}\left(x_1^j,t\right)+I_3\ddot{\psi}_x\left(x_1^j,t\right)\right]\\+\phi_2^j\left(x\right)\left[I_2\ddot{u}\left(x_2^j,t\right)+I_3\ddot{\psi}_x\left(x_2^j,t\right)\right]\\+\phi_3^j\left(x\right)\left[I_2\ddot{u}\left(x_3^j,t\right)+I_3\ddot{\psi}_x\left(x_3^j,t\right)\right]\end{Bmatrix}dx$$

3.3. Consolidated form of Equations

Matrix form of system of equations for boundary nodes i.e. $\xi_k=\left(0,L\right),\ k=\left(1,N\right)$, and domain nodes i.e. $\xi_k=\left(h_e,2h_e,3h_e,...,\left(N-1\right)h_e\right),\ k=\left(2,3,...,N-1\right)$, is given as follows

$$\begin{bmatrix}\mathbf{H}_{uu}^{bb} & \mathbf{H}_{u\psi_x}^{bb} & \mathbf{H}_{u\psi_y}^{bb} & \mathbf{0} & \mathbf{0} & \mathbf{0} & \mathbf{0} & \mathbf{0}\\ \mathbf{H}_{\psi_x u}^{bb}+\mathbf{P}_{\psi_x u}^{bb} & \mathbf{H}_{\psi_x\psi_x}^{bb} & \mathbf{H}_{\psi_x\psi_y}^{bb}+\mathbf{P}_{\psi_x\psi_y}^{bb} & \mathbf{H}_{\psi_x w}^{bb}+\mathbf{P}_{\psi_x w}^{bb} & \mathbf{P}_{\psi_x u}^{bd} & \mathbf{0} & \mathbf{P}_{\psi_x\psi_y}^{bd} & \mathbf{P}_{\psi_x w}^{bd}\\ \mathbf{H}_{\psi_y u}^{bb} & \mathbf{H}_{\psi_y\psi_x}^{bb} & \mathbf{H}_{\psi_y\psi_y}^{bb} & \mathbf{0} & \mathbf{0} & \mathbf{0} & \mathbf{0} & \mathbf{0}\\ \mathbf{0} & \mathbf{P}_{w\psi_x}^{bb} & \mathbf{0} & \mathbf{H}_{ww}^{bb} & \mathbf{0} & \mathbf{P}_{w\psi_x}^{bd} & \mathbf{0} & \mathbf{0}\\ \mathbf{H}_{uu}^{db} & \mathbf{H}_{u\psi_x}^{db} & \mathbf{H}_{u\psi_y}^{db} & \mathbf{0} & \mathbf{I} & \mathbf{H}_{u\psi_x}^{dd} & \mathbf{H}_{u\psi_y}^{dd} & \mathbf{0}\\ \mathbf{H}_{\psi_x u}^{db}+\mathbf{P}_{\psi_x u}^{db} & \mathbf{H}_{\psi_x\psi_x}^{db} & \mathbf{H}_{\psi_x\psi_y}^{db}+\mathbf{P}_{\psi_x\psi_y}^{db} & \mathbf{H}_{\psi_x w}^{db}+\mathbf{P}_{\psi_x w}^{db} & \mathbf{H}_{\psi_x u}^{dd}+\mathbf{P}_{\psi_x u}^{dd} & \mathbf{I} & \mathbf{H}_{\psi_x\psi_y}^{dd}+\mathbf{P}_{\psi_x\psi_y}^{dd} & \mathbf{P}_{\psi_x w}^{dd}\\ \mathbf{H}_{\psi_y u}^{db} & \mathbf{H}_{\psi_y\psi_x}^{db} & \mathbf{H}_{\psi_y\psi_y}^{db} & \mathbf{0} & \mathbf{H}_{\psi_y u}^{dd} & \mathbf{H}_{\psi_y\psi_x}^{dd} & \mathbf{I} & \mathbf{0}\\ \mathbf{0} & \mathbf{P}_{w\psi_x}^{db} & \mathbf{0} & \mathbf{H}_{ww}^{db} & \mathbf{0} & \mathbf{P}_{w\psi_x}^{dd} & \mathbf{0} & \mathbf{I}\end{bmatrix}\begin{Bmatrix}\mathbf{u}^b\\ \boldsymbol{\psi}_x^b\\ \boldsymbol{\psi}_y^b\\ \mathbf{w}^b\\ \mathbf{u}^d\\ \boldsymbol{\psi}_x^d\\ \boldsymbol{\psi}_y^d\\ \mathbf{w}^d\end{Bmatrix}$$

$$=\begin{bmatrix}\mathbf{G}_{uu}^{bb} & \mathbf{0} & \mathbf{0} & \mathbf{0}\\ \mathbf{0} & \mathbf{G}_{\psi_x\psi_x}^{bb} & \mathbf{0} & \mathbf{0}\\ \mathbf{0} & \mathbf{0} & \mathbf{G}_{\psi_y\psi_y}^{bb} & \mathbf{0}\\ \mathbf{0} & \mathbf{0} & \mathbf{0} & \mathbf{G}_{ww}^{bb}\\ \mathbf{G}_{uu}^{db} & \mathbf{0} & \mathbf{0} & \mathbf{0}\\ \mathbf{0} & \mathbf{G}_{\psi_x\psi_x}^{db} & \mathbf{0} & \mathbf{0}\\ \mathbf{0} & \mathbf{0} & \mathbf{G}_{\psi_y\psi_y}^{db} & \mathbf{0}\\ \mathbf{0} & \mathbf{0} & \mathbf{0} & \mathbf{G}_{ww}^{db}\end{bmatrix}\begin{Bmatrix}\mathbf{N}_x^b\\ \mathbf{M}_x^b\\ \mathbf{M}_{xy}^b\\ \mathbf{Q}_{xz}^b\end{Bmatrix}+\begin{Bmatrix}\mathbf{0}\\ \mathbf{0}\\ \mathbf{0}\\ \mathbf{f}^b\\ \mathbf{0}\\ \mathbf{0}\\ \mathbf{0}\\ \mathbf{f}^d\end{Bmatrix}$$

$$+\begin{bmatrix}\mathbf{S}_{uu}^{bb} & \mathbf{S}_{u\psi_x}^{bb} & \mathbf{0} & \mathbf{0} & \mathbf{S}_{uu}^{bd} & \mathbf{S}_{u\psi_x}^{bd} & \mathbf{0} & \mathbf{0}\\ \mathbf{S}_{\psi_x u}^{bb} & \mathbf{S}_{\psi_x\psi_x}^{bb} & \mathbf{0} & \mathbf{0} & \mathbf{S}_{\psi_x u}^{bd} & \mathbf{S}_{\psi_x\psi_x}^{bd} & \mathbf{0} & \mathbf{0}\\ \mathbf{0} & \mathbf{0} & \mathbf{S}_{\psi_y\psi_y}^{bb} & \mathbf{0} & \mathbf{0} & \mathbf{0} & \mathbf{S}_{\psi_y\psi_y}^{bd} & \mathbf{0}\\ \mathbf{0} & \mathbf{0} & \mathbf{0} & \mathbf{S}_{ww}^{bb} & \mathbf{0} & \mathbf{0} & \mathbf{0} & \mathbf{S}_{ww}^{bd}\\ \mathbf{S}_{uu}^{db} & \mathbf{S}_{u\psi_x}^{db} & \mathbf{0} & \mathbf{0} & \mathbf{S}_{uu}^{dd} & \mathbf{S}_{u\psi_x}^{dd} & \mathbf{0} & \mathbf{0}\\ \mathbf{S}_{\psi_x u}^{db} & \mathbf{S}_{\psi_x\psi_x}^{db} & \mathbf{0} & \mathbf{0} & \mathbf{S}_{\psi_x u}^{dd} & \mathbf{S}_{\psi_x\psi_x}^{dd} & \mathbf{0} & \mathbf{0}\\ \mathbf{0} & \mathbf{0} & \mathbf{S}_{\psi_y\psi_y}^{db} & \mathbf{0} & \mathbf{0} & \mathbf{0} & \mathbf{S}_{\psi_y\psi_y}^{dd} & \mathbf{0}\\ \mathbf{0} & \mathbf{0} & \mathbf{0} & \mathbf{S}_{ww}^{db} & \mathbf{0} & \mathbf{0} & \mathbf{0} & \mathbf{S}_{ww}^{dd}\end{bmatrix}\begin{Bmatrix}\ddot{\mathbf{u}}^b\\ \ddot{\boldsymbol{\psi}}_x^b\\ \ddot{\boldsymbol{\psi}}_y^b\\ \ddot{\mathbf{w}}^b\\ \ddot{\mathbf{u}}^d\\ \ddot{\boldsymbol{\psi}}_x^d\\ \ddot{\boldsymbol{\psi}}_y^d\\ \ddot{\mathbf{w}}^d\end{Bmatrix} \tag{83}$$

In the above system of equations, quantities related to boundary and domain nodes are specified by the use of superscripts **b** and **d**. In the coefficient matrices containing double superscripts, first one indicates the source or fixed point and second indicates the field point. Different entries of coefficient matrices in Eq. (83) are sub-matrices for e.g. **P** and **S** are sub-matrices and are produced by domain integrals given in Appendix A. $\mathbf{Q_{xz}}$, $\mathbf{M_{xy}}$, $\mathbf{M_x}$ and $\mathbf{N_x}$ are transverse shear force, twisting moment, bending moment and axial force respectively. Loading vector, zero matrix and identity matrix are denoted by **f**, **0** and **I**. **H** and **G** sub-matrices are given in Appendix B.

3.4. Load Vector

Load vector in Eq. (83) is evaluated depending on the type of the applied load. In case of distributed load on LCB, load integral in Eq. (79d) gives the following expression

$$\mathbf{f}^{\mathrm{b}} = -\frac{qL^2}{4\bar{A}_{55}}\begin{Bmatrix}1\\1\end{Bmatrix} \qquad \mathbf{f}^{\mathrm{d}} = -\frac{q}{4\bar{A}_{55}}\begin{Bmatrix}\xi_2^2+\left(L-\xi_2\right)^2\\ \xi_3^2+\left(L-\xi_3\right)^2\\ \vdots\\ \xi_{N-1}^2+\left(L-\xi_{N-1}\right)^2\end{Bmatrix} \tag{84}$$

Load vector, in case of concentrated load at a point $x = x_p$, is given as follows

$$\mathbf{f}^{\mathrm{b}} = \frac{P}{2\bar{A}_{55}}\begin{Bmatrix}-x_p\\ x_p-L\end{Bmatrix} \qquad \mathbf{f}^{\mathrm{d}} = -\frac{P}{2\bar{A}_{55}}\begin{Bmatrix}|\xi_2-x_p|\\ |\xi_3-x_p|\\ \vdots\\ |\xi_{N-1}-x_p|\end{Bmatrix} \tag{85}$$

Time derivatives of unknown quantities in Eq. (83) are approximated via Houbolt method [30]. In this method, temporal variation of a parameter is estimated from $t = t_{\mathrm{n-2}}$ to $t = t_{\mathrm{n+1}}$ via cubic Lagrange interpolation. Based on this method, approximation of first and second order derivatives can be performed as follows

$$\dot{y}_{n+1} = \frac{1}{6\Delta t}\left\{11y_{n+1}-18y_n+9y_{n-1}-2y_{n-2}\right\} \tag{86}$$

$$\ddot{y}_{n+1} = \frac{1}{\Delta t^2}\{2y_{n+1} - 5y_n + 4y_{n-1} - y_{n-2}\} \tag{87}$$

Eq. (83) is implemented in MATLAB for revealing the dynamic response of LCB.

CHAPTER 4

NUMERICAL RESULTS

5.1. Validation

In order to validate the numerical results obtained from D-BEM, undamped forced vibration response of an homogeneous isotropic Timoshenko beam is compared to analytical solutions, developed by Garcia et al. [31], for a simply supported homogeneous isotropic beam. Following are the material and geometric properties of the homogeneous isotropic beam.

Table 1: Properties of homogeneous Timoshenko beam

No.	Property	Value	Units
1	E	50	[GPa]
2	G	20.833	[GPa]
3	v	0.2	-
4	ρ	2500	[kg/m^3]
5	k_s	5/6	-
6	L	200	[mm]
7	b	20	[mm]
8	h	16	[mm]

Dynamic loads, used in comparison, are given as follows:

$$q = P\delta\left(x - x_p\right)H\left(t\right) \qquad \text{Point step force} \qquad (88a)$$

$$q = P\delta\left(x - x_p\right)\sin\left(\omega t\right) \qquad \text{Point Harmonic force} \qquad (88b)$$

$$q = q_0 H\left(t\right) \qquad \text{Uniformly Distributed Step force} \qquad (88c)$$

$$q = P\delta\left(x - x_p\right)\delta\left(t\right) \qquad \text{Impulse force} \qquad (88d)$$

Variation of midpoint's deflection $w(L/2, t)$ and pinned-pinned boundary condition are used for comparing D-BEM results with analytical solutions.

5.1.1. Analytical Solutions

For a simply supported homogeneous isotropic beam, following form of analytical solutions is assumed by employing separation of variables technique [1].

$$w\left(x,t\right) = \sum_{m=1,3,5}^{\infty} W_m\left(t\right)\sin\left(\frac{m\pi x}{L}\right) \qquad (89a)$$

$$\psi_x\left(x,t\right) = \sum_{m=1,3,5}^{\infty} Q_m\left(t\right)\cos\left(\frac{m\pi x}{L}\right) \qquad (89b)$$

Following expression is found for $W_m\left(t\right)$ [1, 31]

$$W_m\left(t\right) = \left\{\rho I\ddot{Q}_m\left(t\right) + \left[EI\left(\frac{m\pi}{L}\right)^2 + k_s GA\right]Q_m\left(t\right)\right\}\frac{1}{k_s GA\left(\frac{m\pi}{L}\right)} \qquad (90)$$

The term $\ddot{Q}_m\left(t\right)$ is second order time derivative of $Q_m\left(t\right)$ which is dependent on the type of dynamic load acting on the structure. For uniformly distributed step load $q = q_0 H\left(t\right)$, it is given by:

$$Q_m\left(t\right) = \frac{4qL^3}{EI\left(m\pi\right)^4\left(\delta_m^2 - \theta_m^2\right)}\left[\theta_m^2\cos\left(\delta_m t\right) - \delta_m^2\cos\left(\theta_m t\right) + \left(\delta_m^2 - \theta_m^2\right)\right] \qquad (91)$$

For concentrated step load $q = P\delta\left(x - x_p\right)H\left(t\right)$, where x_p is the point of application, the expression for $Q_m\left(t\right)$ is as follows:

$$Q_m(t) = \frac{2PL^2 \sin\left(\frac{m\pi x_p}{L}\right)}{EI(m\pi)^3\left(\delta_m^2 - \theta_m^2\right)}\left[\theta_m^2 \cos(\delta_m t) - \delta_m^2 \cos(\theta_m t) + \left(\delta_m^2 - \theta_m^2\right)\right] \tag{92}$$

In case of point harmonic force at $x = x_p$ and having a frequency $\omega = \omega_p$, the expression for $Q_m(t)$ is given by:

$$Q_m(t) = \frac{2P(m\pi)}{L^2\left(\frac{\rho^2 I}{k_s G}\right)}\left\{\begin{array}{l}\frac{\omega_p}{\left(\delta_m^2 - \theta_m^2\right)}\left[\frac{\sin(\theta_m t)}{\theta_m\left(\omega_p^2 - \theta_m^2\right)} - \frac{\sin(\delta_m t)}{\delta_m\left(\omega_p^2 - \delta_m^2\right)}\right] \\ + \frac{\sin(\omega_p t)}{\left(\omega_p^2 - \theta_m^2\right)\left(\omega_p^2 - \delta_m^2\right)}\end{array}\right\}\sin\left(\frac{m\pi x_p}{L}\right) \tag{93}$$

For impulsive excitation at $x = x_p$ and $t = 0$, the expression for $Q_m(t)$ is:

$$Q_m(t) = \frac{2P(m\pi)}{L^2\left(\frac{\rho^2 I}{k_s G}\right)}\left[\frac{\sin(\theta_m t)}{\theta_m} - \frac{\sin(\delta_m t)}{\delta_m}\right]\sin\left(\frac{m\pi x_p}{L}\right)\left(\frac{1}{\delta_m^2 - \theta_m^2}\right) \tag{94}$$

where

$$\theta_m = \sqrt{\alpha_m - \beta_m} \tag{95a}$$

$$\delta_m = \sqrt{\alpha_m + \beta_m} \tag{95b}$$

and

$$\alpha_m = \frac{\rho A + \rho I\left(1 + \frac{E}{k_s G}\right)\left(\frac{m\pi}{L}\right)^2}{2\left(\frac{\rho^2 I}{k_s G}\right)} \tag{96a}$$

$$\beta_m = \frac{\sqrt{(\rho A)^2 + 2(\rho A)(\rho I)\left(1 + \frac{E}{k_s G}\right)\left(\frac{m\pi}{L}\right)^2 + (\rho I)^2\left(1 - \frac{E}{k_s G}\right)^2\left(\frac{m\pi}{L}\right)^4}}{2\left(\frac{\rho^2 I}{k_s G}\right)} \tag{96b}$$

5.1.2. D-BEM and Analytical solution comparison

5.1.2.1. Distributed Step Load

Comparison of results, obtained from D-BEM formulation, with analytical solution is shown in Fig. 5. Discretization scheme, time step of the analysis and magnitude of the uniformly distributed step load is given as follows

Table 2: Distributed step load analysis validation parameters

No.	Parameter	Value
1	Number of cells	16
2	Time Step	$4(10^{-5})$ [s]
3	Load Magnitude	5 [kN/m]

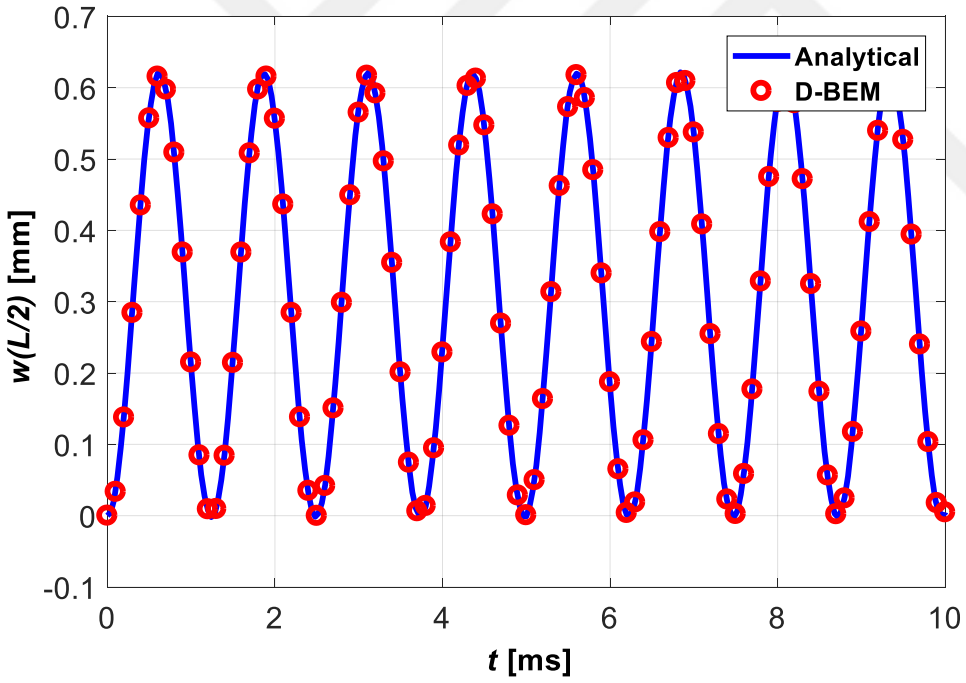

Figure 5: Response Comparison in case of Distributed Step load

Excellent agreement is observed between D-BEM and closed form solution, reflecting the high degree of accuracy achieved by D-BEM.

5.1.2.2. Concentrated Step Load

Fig. 6 shows the comparison between the result obtained from D-BEM formulation and analytical solution. Number of cells, time step of the analysis and magnitude of the concentrated step load is given as follows

Table 3: Concentrated Step load analysis validation parameters

No.	Parameter	Value
1	Number of cells	16
2	Time Step	$4(10^{-5})$ [s]
3	Load Magnitude	0.5 [kN]

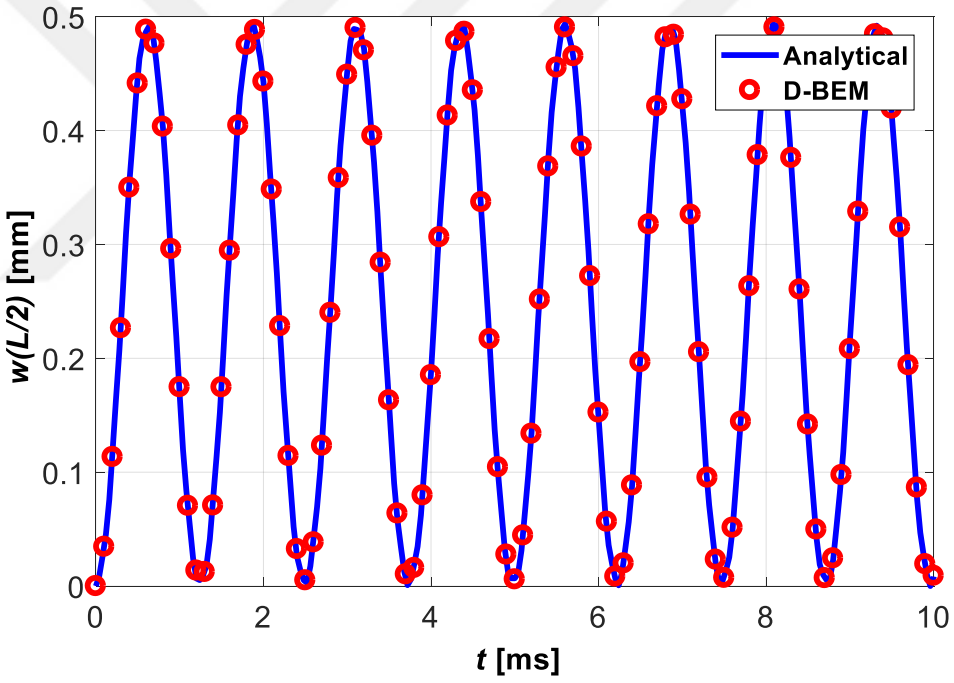

Figure 6: Response comparison in case of Concentrated Step load

Perfect agreement is observed between the D-BEM and analytical solution, indicating the high degree of accuracy achieved by D-BEM.

5.1.2.3. Concentrated Harmonic Load

For harmonic load, comparison between the result obtained from D-BEM formulation and analytical solution is shown in Fig. 7. Time step, number of cells, frequency and magnitude of the harmonic load are given as follows

Table 4: Concentrated harmonic load analysis validation parameters

No.	Parameter	Value
1	Number of cells	16
2	Time Step	$4(10^{-5})$ [s]
3	Load Magnitude	1 [kN]
4	Load Frequency	500 [rad/s]

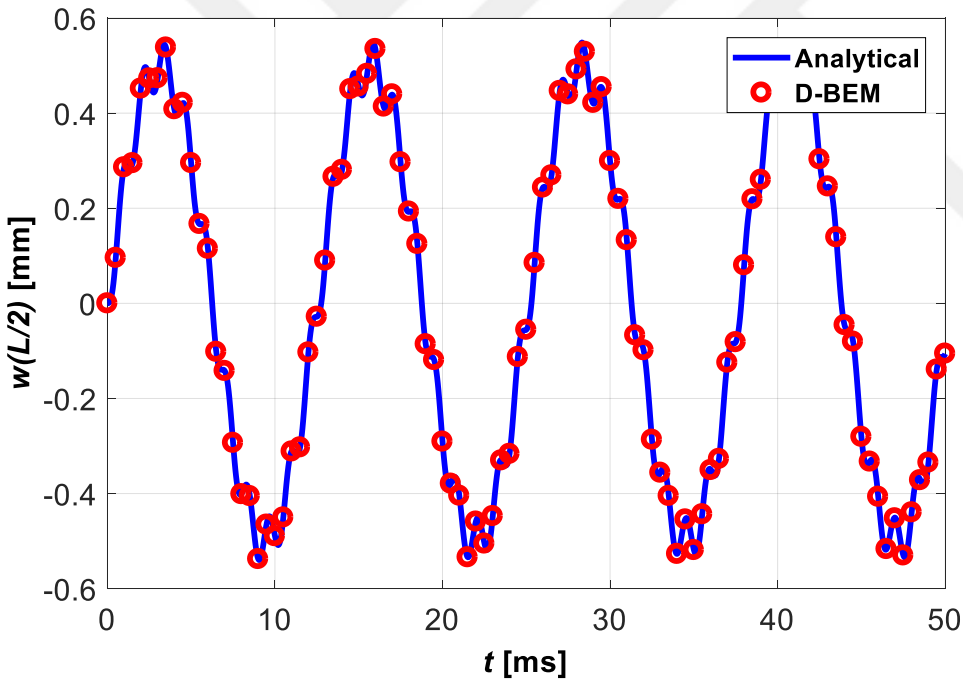

Figure 7: Response Comparison in case of Concentrated Harmonic load

Close agreement observed between the D-BEM and analytical solution indicates the accuracy achieved by the developed technique.

5.1.2.4. Impulsive Load

Fig. 8 shows the comparison of time variation of transverse deflection obtained via D-BEM and analytical solution. Table 5 contains the values of analysis parameters used for obtaining the dynamic response via D-BEM.

Table 5: Impulse load analysis validation parameters

No.	Parameter	Value
1	Number of cells	64
2	Time Step	$1(10^{-6})$ [s]
3	Load Magnitude	0.5 [N.s]

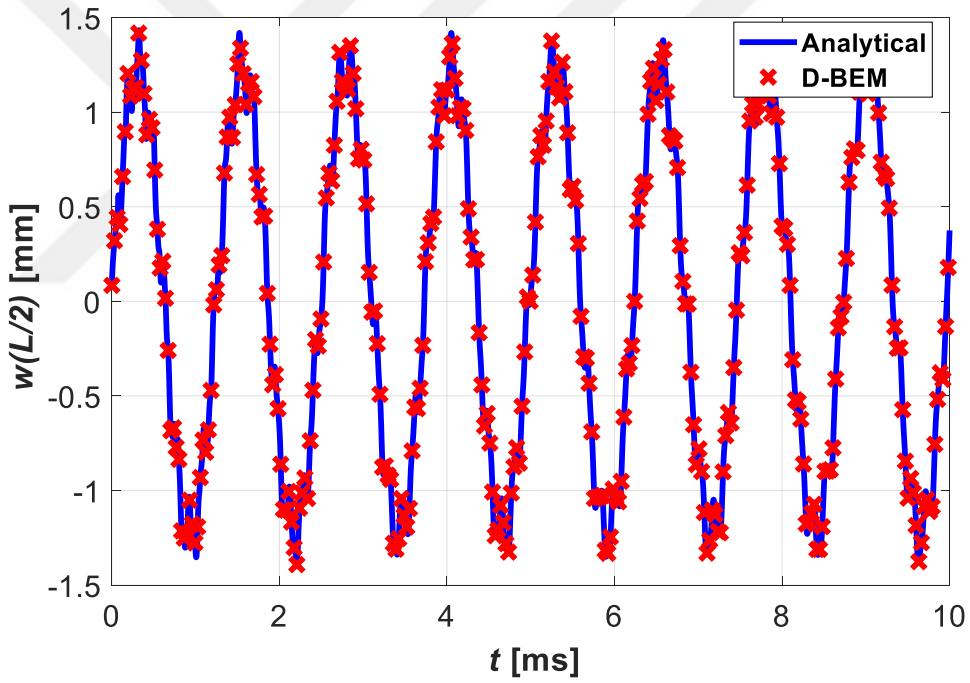

Figure 8: Response Comparison in case of Impulse load

Comparison indicates that results obtained from D-BEM are highly accurate.

5.2. Convergence Study and Parametric Analyses

General geometry of LCB, examined in parametric analyses is shown in Fig. 1. AS4/3501 graphite-epoxy is used as material for constituent laminas whose orthotropic properties are given below:

Table 6: Material properties of AS4/3501 Graphite-Epoxy [20]

No.	Property	Value	Units
1	E_{11}	144.8	[GPa]
2	E_{22}	9.65	[GPa]
3	G_{12}	4.14	[GPa]
4	G_{13}	4.14	[GPa]
5	G_{23}	3.45	[GPa]
6	v_{12}	0.33	-
7	ρ	1389.23	[kg/m^3]

Two different groups of LCBs are studied, which are named as LCB-1 and LCB-2. Overall dimensions of both LCBs are same and, their length, width and total thickness are equal to 200 mm, 20 mm and 16 mm respectively. Major difference between the two LCBs is lamina thickness. A total of four laminas, having a thickness of 4 mm each, are used in constructing LCB-1. On the other hand, LCB-2 contains eight laminas having same thickness of 2 mm. Each type is further sub-divided into four configurations and a total of eight configurations are analyzed in the parametric analyses. Different configurations of LCBs arise from variation in orientation of fiber angle and stacking arrangement of laminas. Variation of transverse deflection of midpoint and normal axial stress at midpoint of top surface of all configurations, with time, are studied under the action of time based loads. Results are compared, under same load conditions, to assess the performance of all

configurations. Details of the configurations of LCB-1 and LCB-2 examined in parametric analyses are given in Table 7 and 8, respectively.

Table 7: LCB-1 Configurations

No.	Configuration	Sequence	Notation
1	Cross-ply	$[0/90]_2$	CP1
2	Symmetric cross-ply	$[0/90]_s$	CP2
3	Symmetric Angle-ply	$[45/-45]_s$	AP1
4	Anti-symmetric Angle-ply	$[45/-45]_2$	AP2

Table 8: LCB-2 Configurations

No.	Configuration	Sequence	Notation
1	Cross-ply	$[0/90]_4$	CP3
2	Symmetric cross-ply	$[0/90/0/90]_s$	CP4
3	Symmetric Angle-ply	$[45/-45/45/-45]_s$	AP3
4	Anti-symmetric Angle-ply	$[45/-45]_4$	AP4

5.2.1. Convergence Analyses

In order to investigate the convergence characteristics of D-BEM, undamped dynamic response of configuration CP2 is analyzed under the action of uniformly distributed step load of magnitude q_0 = 50 kN/m. Fig. 9 shows the response $w(L/2, t)$ of LCB-CP2 to time dependent load. M denotes the number of cells used for discretization. Time step is specified as 10^{-5} s for all values of M.

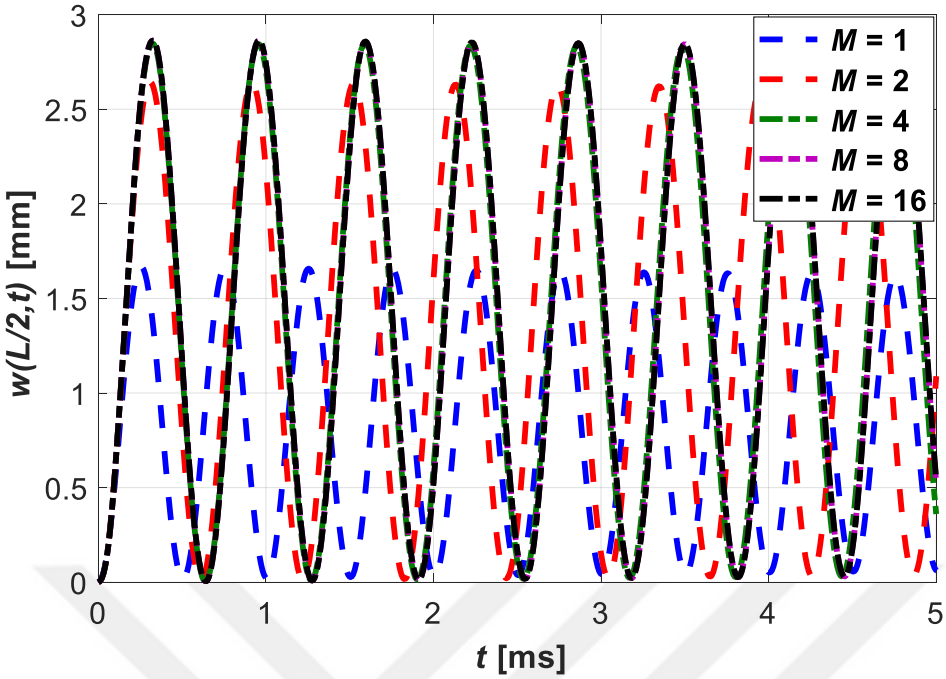

Figure 9: Convergence Study - Distributed Step load for CP2

Percentage difference (*PD*) values between deflection values, at certain points in time, under different values of *M* are given in Table 9. *PD* values between two consecutive cell counts, at same time, are used to check if the convergence is established. It is calculated as follows:

$$PD = \frac{|w(M=4) - w(M=2)| * 100}{|w(M=2)|} \tag{97}$$

Table 9: Convergence Study- Distributed Step load for CP2

***t* [s]**	***M* (Number of cells)**				
	1	**2**	**4**	**8**	**16**
0,005	w = 0,06	w = 1,08	w = 0,36	w = 0,53	w = 0,54
		PD = 1639	PD = 66,2	PD = 46,6	PD = 2,4
0,01	w = 0,11	w = 2,51	w = 1,14	w = 1,61	w = 1,64
		PD = 2196	PD = 54,4	PD = 40,9	PD = 1,97
0,015	w = 0,15	w = 1,88	w = 2,01	w = 2,53	w = 2,56
		PD = 1120	PD = 6,67	PD = 26,3	PD = 1,1
0,02	w = 0,19	w = 0,35	w = 2,6	w = 2,7	w = 2,69
		PD = 81,6	PD = 626	PD = 4,8	PD = 0,47
0,025	w = 0,24	w = 0,54	w = 2,67	w = 2,07	w = 2,01
		PD = 128	PD = 395	PD = 22,1	PD = 3,1
0,03	w = 0,27	w = 2,03	w = 2,2	w = 1,06	w = 0,98
		PD = 640	PD = 10,6	PD = 52,3	PD = 7,57
0,035	w = 0,31	w = 2,26	w = 1,5	w = 0,34	w = 0,30
		PD = 630	PD = 33,4	PD = 77,6	PD = 11,5
0,04	w = 0,3	w = 0,92	w = 0,76	w = 0,32	w = 0,37
		PD = 166,7	PD = 16,2	PD = 56,9	PD = 13,7

It is shown in Fig. 9 and Table 9 that D-BEM results converge at $M = 16$.

In the case of LCB-1-CP2 subjected to impulsive load of magnitude P = 0.5 N.s, it has been shown in Fig. 10 and Table 10 that D-BEM establishes convergence when the time step is equal to 10^{-6} s and number of cells is specified as 64.

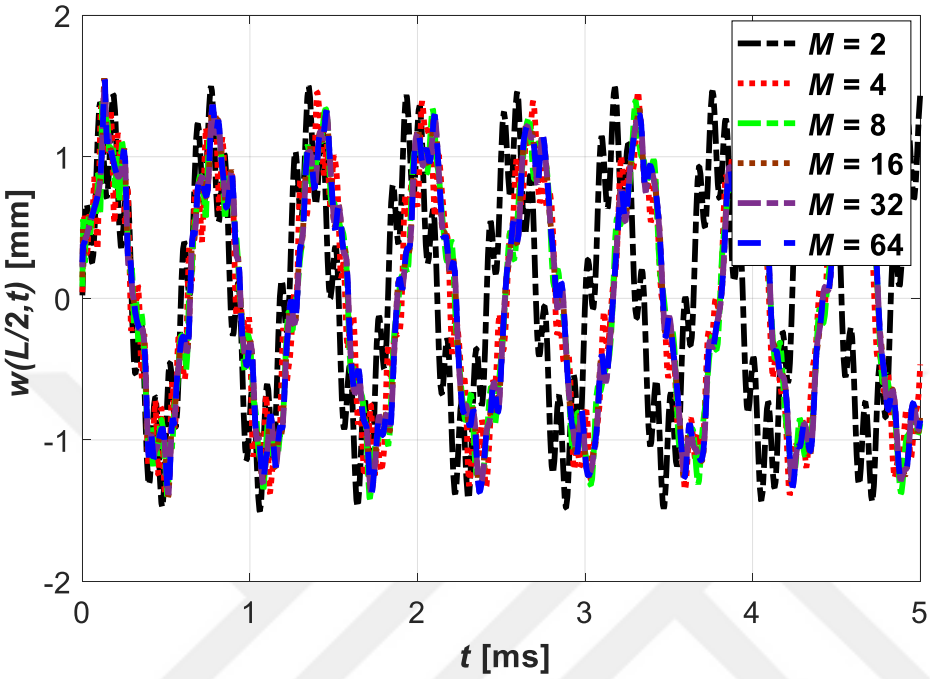

Figure 10: Convergence Study - Impulsive load for CP2

Table 10: Convergence Study - Impulsive load for CP2

***t* [s]**	***M* (Number of cells)**					
	2	**4**	**8**	**16**	**32**	**64**
0,005	*w* = 1,43	*w* = -0,48	*w* = -0,89	*w*= -0,84	*w* = -0,87	*w* = -0,87
		PD=133,7	*PD* = 85,2	*PD*= 5,6	*PD*= 3,17	*PD*= 0,09
0,01	*w* = 0,04	*w* = -0,78	*w* = -1,2	*w*= -0,97	*w* = -0,9	*w* = -0,9
		PD=2106	*PD* = 51,9	*PD*= 19	*PD*= 1,62	*PD*= 0,10
0,015	*w* = -1,1	*w* = -0,93	*w* = -0,96	*w* = -0,9	*w* = -1,0	*w* = -1,0
		PD= 15,2	*PD* = 4,3	*PD* = 2,1	*PD* = 5,4	*PD* = 0,3
0,02	*w* = 0,19	*w* = -0,9	*w* = -0,54	*w*=-0,83	*w* = -0,87	*w* = -0,87
		PD = 584	*PD* = 41,7	*PD*=54	*PD* = 4,8	*PD*= 0,15
0,025	*w* = 0,75	*w* = -0,77	*w* = -0,08	*w*= -0,07	*w* = -0,05	*w* = -0,05
		PD = 202	*PD* = 88,8	*PD*= 19	*PD*= 18,3	*PD* = 3,8
0,03	*w* = -0,6	*w* = -0,48	*w* = 0,40	*w*= 0,79	*w* = 0,77	*w* = 0,77
		PD= 19,3	*PD*= 182,9	*PD*=96,9	*PD* = 2,7	*PD*= 0,02
0,035	*w* = -0,6	*w* = -0,09	*w* = 0,89	*w* = 1,01	*w* = 0,95	*w* = 0,95
		PD= 83,8	*PD* = 1047	*PD* = 12	*PD* = 5,2	*PD*= 0,16
0,04	*w* = 0,97	*w* = 0,32	*w* = 1,17	*w*= 0,96	*w* = 0,98	*w* = 0,99
		PD= 66,8	*PD*= 262,6	*PD* = 17	*PD*= 2,43	*PD*= 0,33

5.2.2. Parametric Analyses

In parametric analyses, undamped forced vibration response of LCB-1 and LCB-2 is studied. For step and harmonic loadings, 16 cells and a time step of 10^{-5} s was specified and for impulsive load, a time step of 10^{-6} s and 64 cells were used for domain discretization in the parametric analyses. Load magnitude selection is based on two main factors i.e. applicability of small strain theory and possibility of application of loads in experimental setup. Maximum deflection and stress values, experienced by the structure in parametric analyses, are observed to be in accordance with the small strain theory. Secondly, the specified forces can be easily applied to the structure in experimental setting by using a medium-force shaker such as LDS V875LS by Brüel and Kjaer.

5.2.2.1. Step Loading

Time variation of transverse displacement and longitudinal stress, of LCB-1's configurations, in response to uniformly distributed step load are shown in Fig. 11 and 12 respectively. Distributed load has a magnitude of q_0 = 5 kN/m.

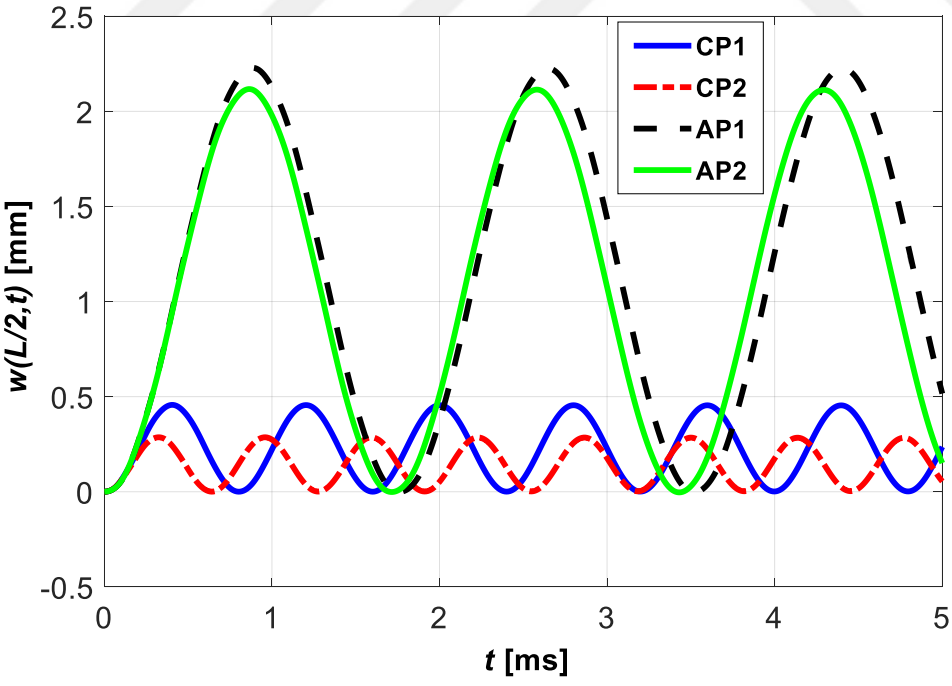

Figure 11: Deflection response LCB-1: Distributed Step load q_0 = 5 kN/m

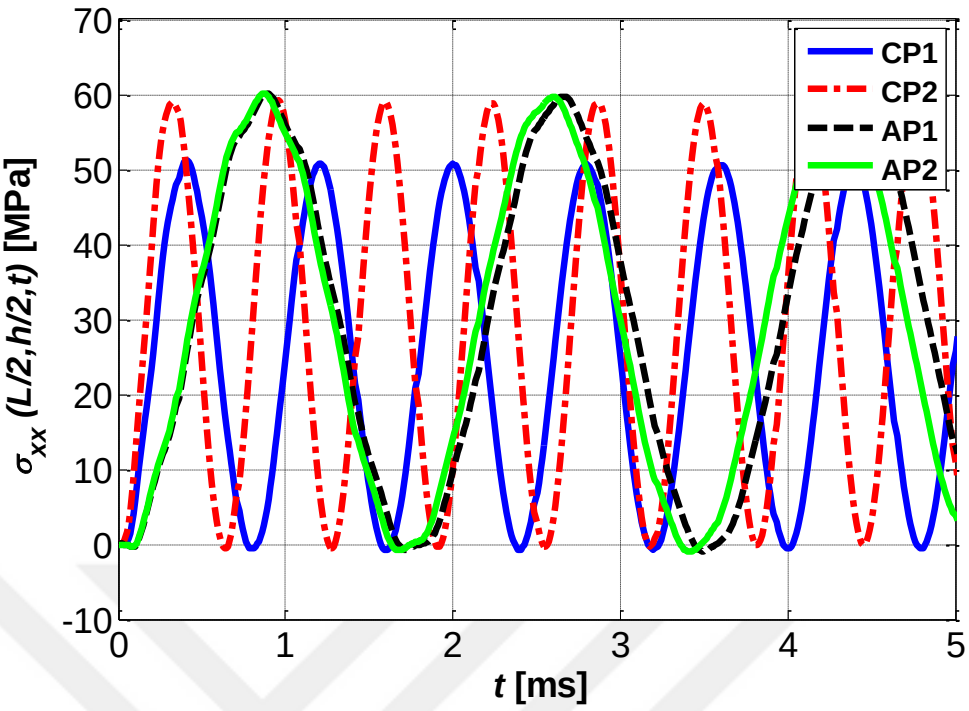

Figure 12: Normal axial stress response LCB-1: Distributed Step load q_0 = 5 kN/m

Time history plots of deflection and axial stress, for four configurations of LCB-2 when subjected to distributed step load of magnitude q_0 = 5 kN/m, are shown in Fig. 13 and 14 respectively.

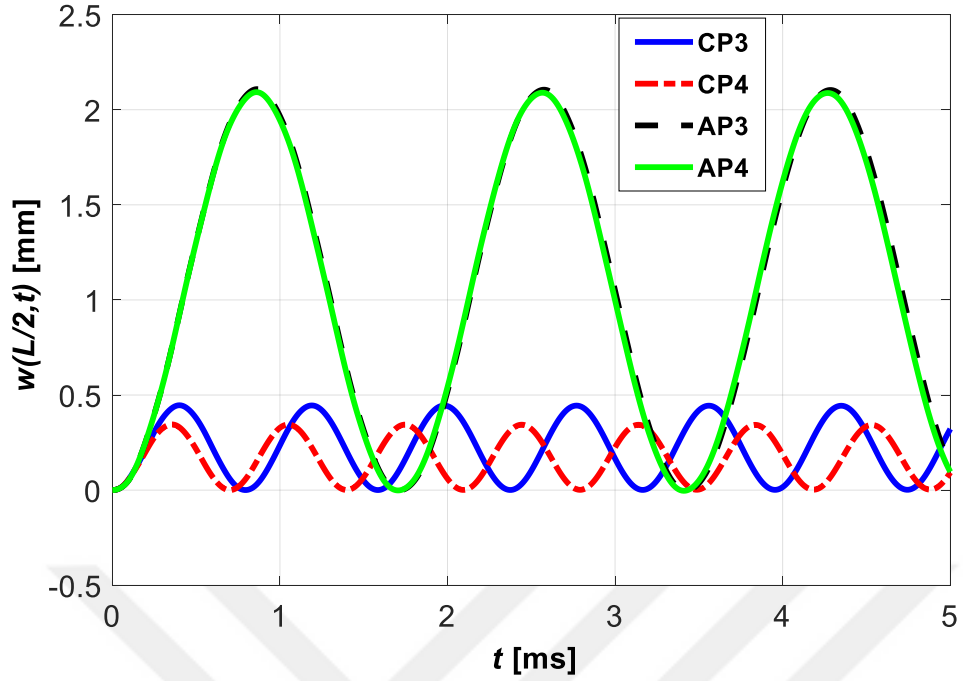

Figure 13: Deflection response LCB-2: Distributed Step load q_0 = 5 kN/m

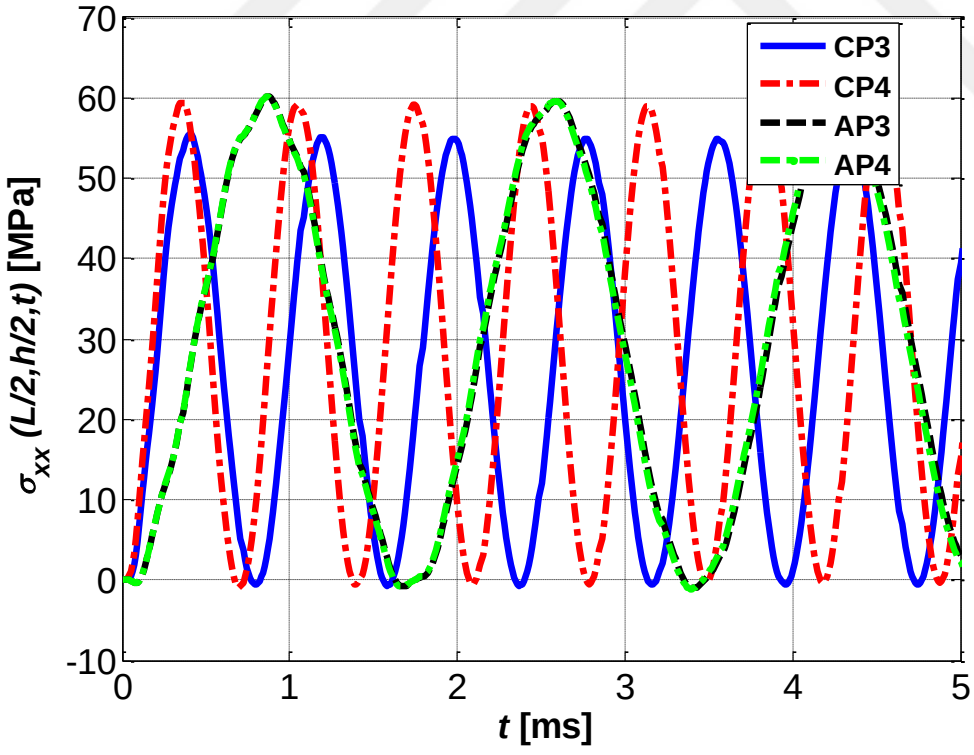

Figure 14: Normal axial stress response LCB-2: Distributed Step load q_0 = 5 kN/m

Harmonic response of transverse deflection in Figs. 11 and 13 is attributed to the fact that structures vibrate with their first natural frequency when subjected to step loads. Based on this, it can be inferred that angle-ply LCBs have lower first natural frequency than cross-ply LCBs. Figs. 11 and 13 show that angle-ply configurations of both LCBs undergo large deflections as compared to cross-ply configurations. By comparing the stress results in Figs. 12 and 14, it can be seen that lowest stress magnitudes are experienced by cross-ply configuration LCB-1-CP1. Stresses generated in all other configurations, of both LCBs, are found to be close in magnitude to each other and greater in magnitude than those calculated for CP1. It can be deduced; from Figs. 11 and 13, that cross-ply configuration LCB-1-CP1 will be better suited to the applications where maximum deflection is a constraint due to its lowest deflection as compared to other configurations. It can also be inferred from axial stress results, in Figs. 12 and 14, that CP1 configuration of LCB-1 will be more resilient to failure as compared to other configurations of both LCBs.

Time response of transverse deflection of four configurations of both LCB-1 and LCB-2, mentioned in Table 7 and 8, to concentrated step load is shown in Figs. 15 and 16 respectively. Magnitude of point step load used to excite the structure is P = 0.5 kN. Transverse deflection response, in case of this load, is cyclic in nature and has constant amplitude. Smallest deflection is observed for CP1 configuration of LCB-1, rendering it the best choice for applications requiring low maximum deflection. Figs. 17 and 18 show the axial stress response, to concentrated step load of magnitude 0.5 kN, of all configurations of LCB-1 and LCB-2 respectively. It can be seen, in Figs. 17 and 18, that normal stress generated in CP1 has the lowest value and hence will be less prone to failure as compared to other configurations.

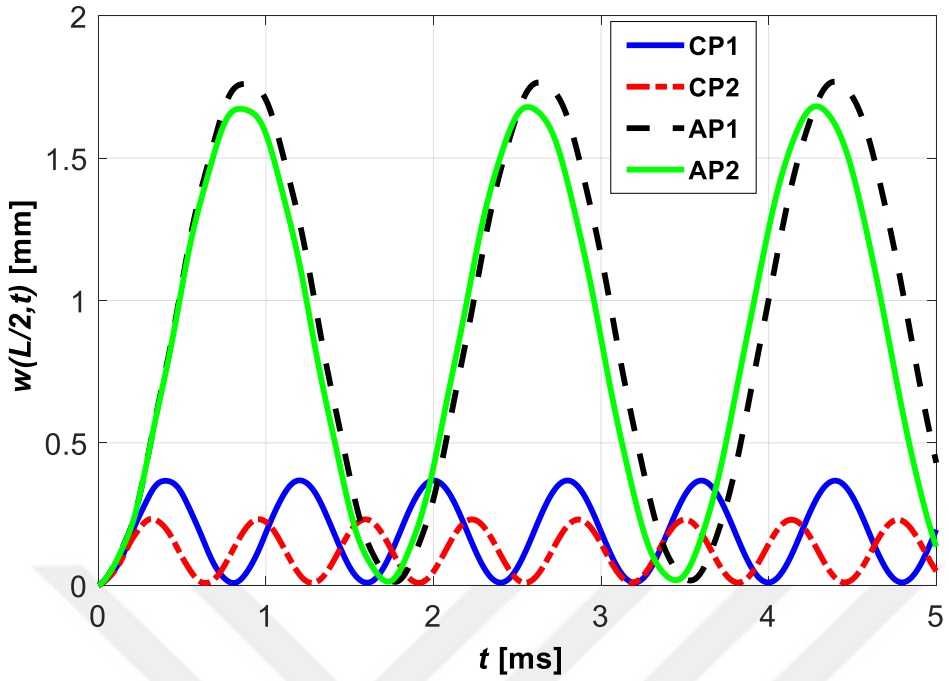

Figure 15: Deflection response LCB-1: Concentrated Step load P = 0.5 kN at x_p = L/2

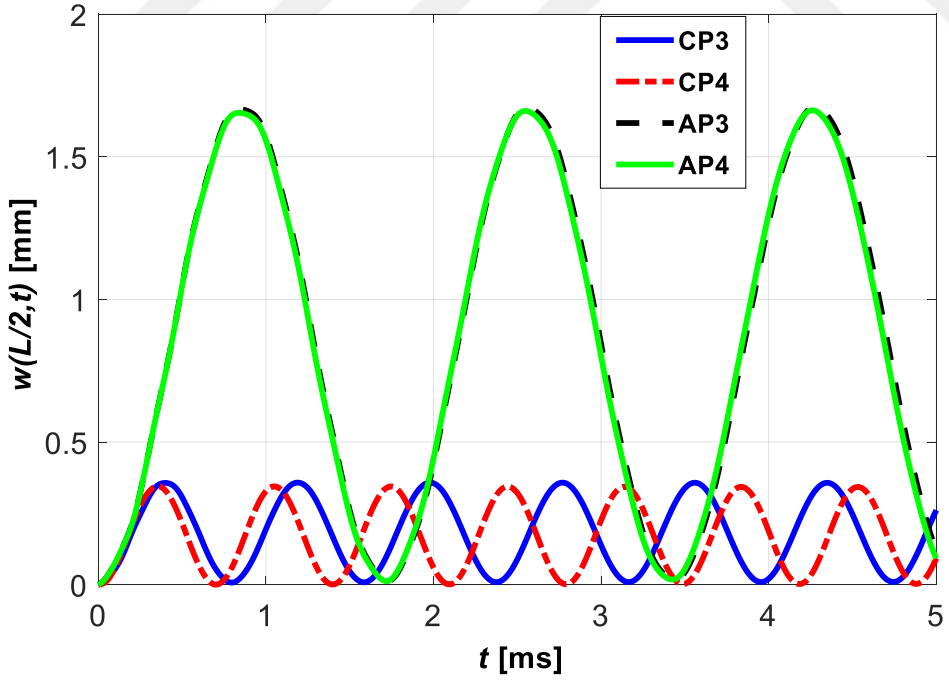

Figure 16: Deflection response LCB-2: Concentrated Step load P = 0.5 kN at x_p = L/2

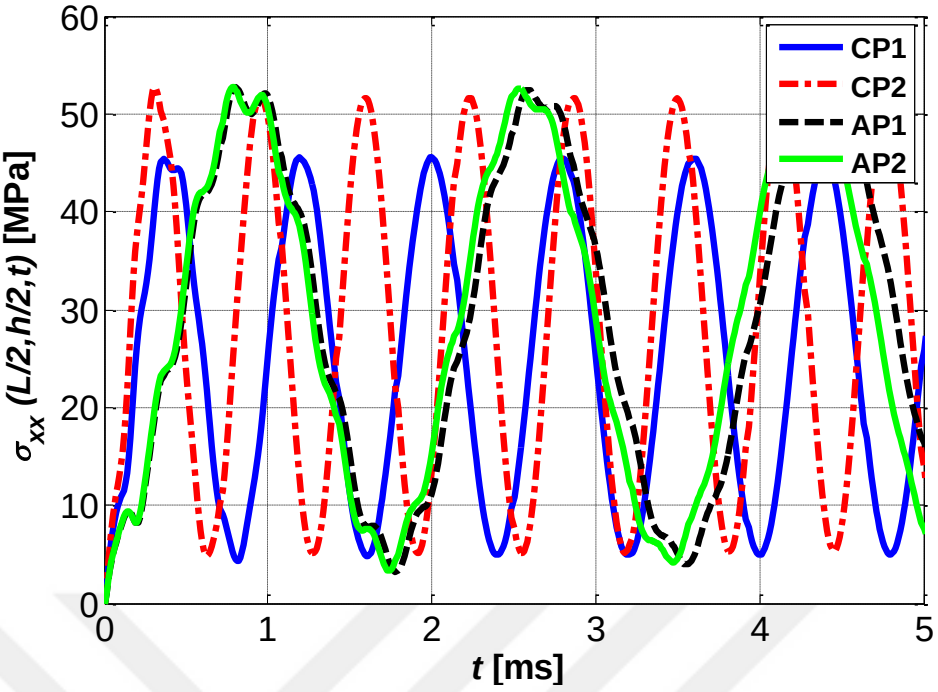

Figure 17: Axial stress response LCB-1: Concentrated Step load P = 0.5 kN at x_p = L/2

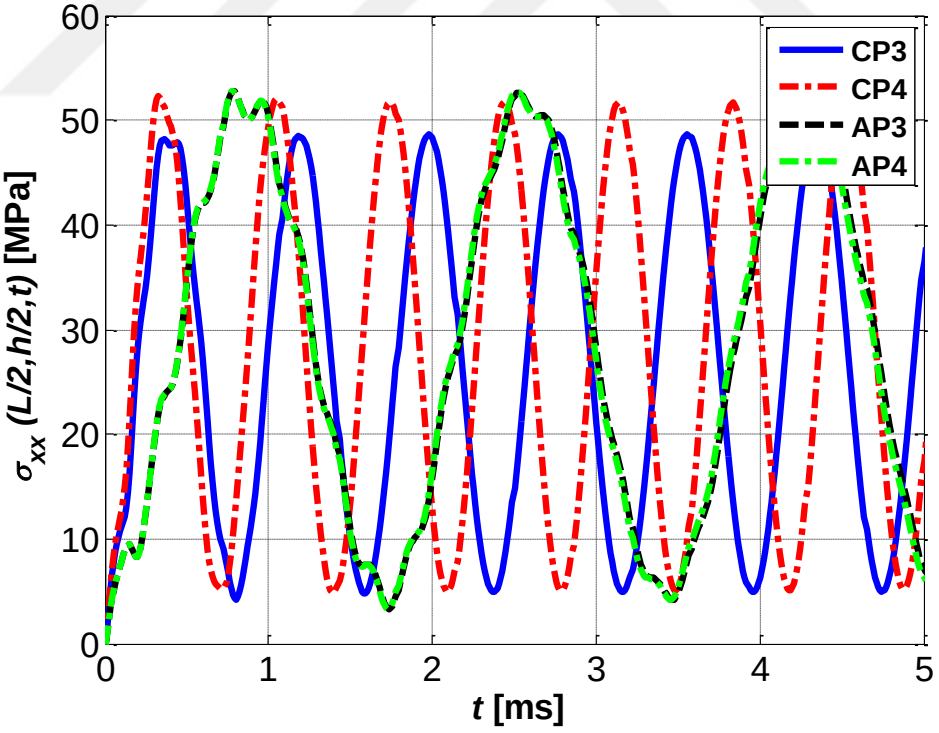

Figure 18: Axial stress response LCB-2: Concentrated Step load P = 0.5 kN at x_p = L/2

By comparing the deflection response of cross-ply configurations of LCB-1 i.e. CP1 and CP2 to each other, for instance in Fig. 15, influence of lamina lay-up or stacking sequence can be observed. For example, by comparing the response of CP1 and CP2 it can be observed that they have different response to external force of same magnitude despite having layers with same geometric dimensions and fiber angle. The reason for this behavior is the stacking arrangement of laminas as this affects the material response couplings when subjected to external force. CP1 and CP2 are cross-ply configurations having two 0 and two 90 degree fiber angle laminas. For both configurations there is no coupling in response between twist-bending and twist-extension. But due to symmetric nature of lamina stacking, about geometric midplane, in CP2, there is also no coupling in response between extension and bending. This leads to different vibration frequency and amplitude under distributed and point step loads of same magnitude. Similarly, the difference in response of angle-ply configurations, in Fig. 15, is the aftermath of stacking arrangement of laminas. For LCB-2, similar effect of stacking arrangement of laminas can also be observed in Figs. 13 and 16.

5.2.2.2. Harmonic Load

Figs. 19 and 20 show the time variation plots of transverse deflection response, of all configurations of LCB-1 and LCB-2, to concentrated harmonic excitation, respectively. Magnitude and frequency of the applied load are P = 1.0 kN and ω_p = 500 rad/s. In the case of harmonic force, vibration frequency of a structure is the same as the frequency of applied force. Therefore, in Figs. 19 and 20, all configurations have same frequency of vibration. Due to the inclusion of free vibration frequencies in the forced response, small perturbations can be observed in Figs. 19 and 20. The difference in amplitude of vibration, under harmonic load, follows the same trend as was observed under the action of step loads i.e. angle-ply configurations experience larger deflections than cross-ply configurations of both LCBs. Cross-ply configurations of both LCB-1 and LCB-2 are more stiff as compared to angle-ply configurations and will be more suitable to applications which require low deflections.

Figs. 21 and 22 show the axial stress response of all configurations of LCB-1 and LCB-2 respectively. It can be observed that normal stress values, of all configurations, generally vary close to each other.

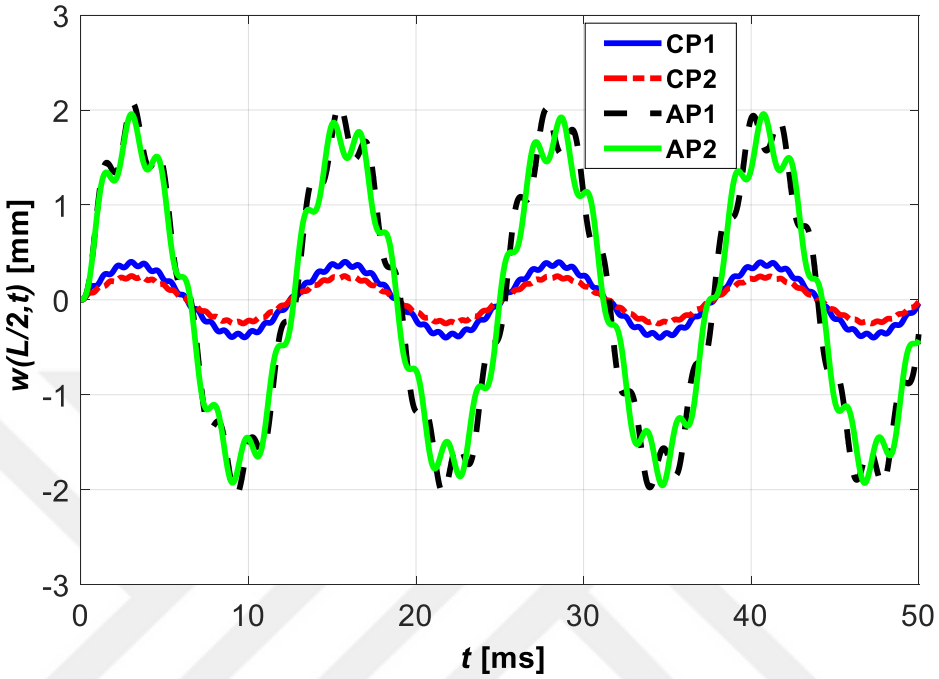

Figure 19: Deflection response LCB-1: Harmonic load P = 1.0 kN and ω_p = 500 rad/s at x_p= L/2

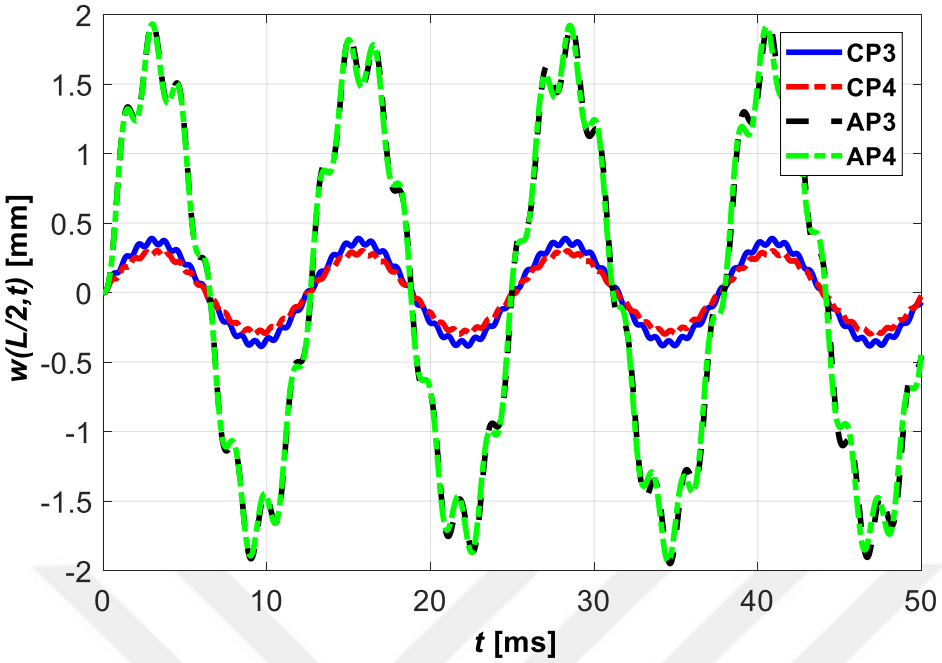

Figure 20: Deflection response LCB-2: Harmonic load P = 1.0 kN and ω_p = 500 rad/s at x_p= L/2

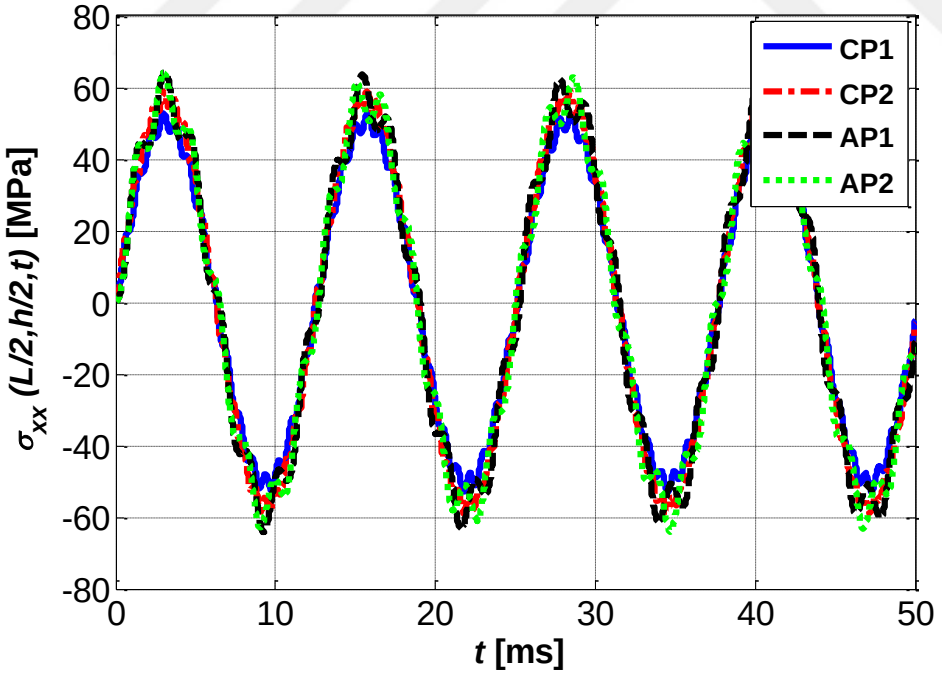

Figure 21: Axial stress response LCB-1: Harmonic load P = 1.0 kN and ω_p = 500 rad/s at x_p= L/2

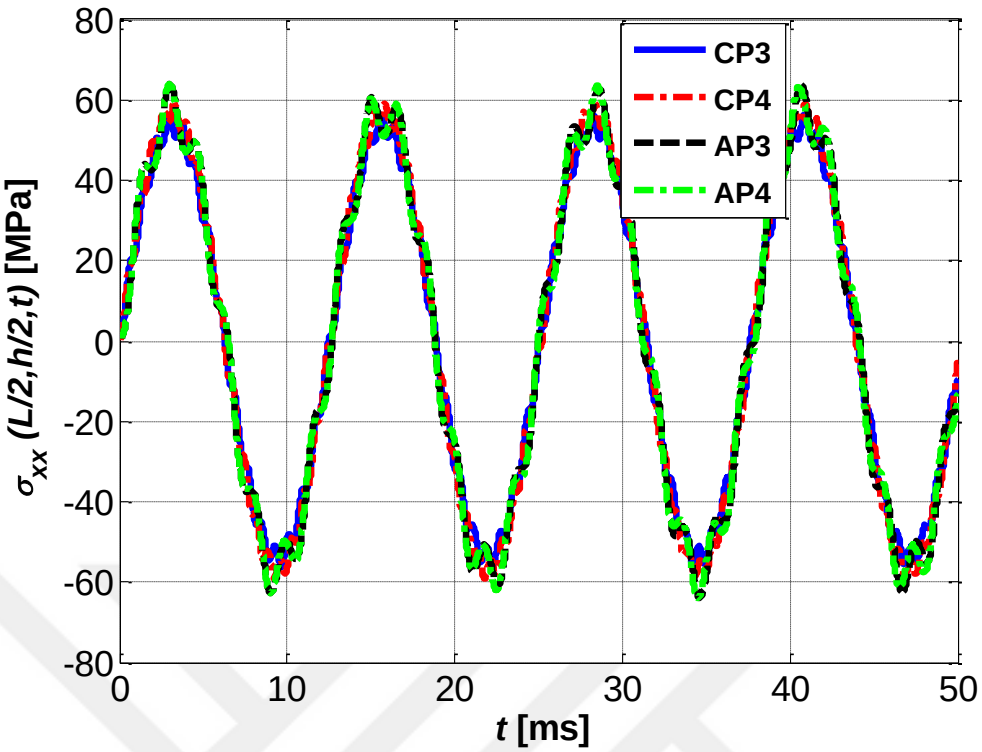

Figure 22: Axial stress response LCB-2: Harmonic load P = 1.0 kN and ω_p = 500 rad/s at x_p= L/2

Differences in amplitude of vibration between CP1-CP2 and between AP1-AP2 configurations of LCB-1, shown in Fig. 19, are resulting from stacking arrangement of laminas due to its influence on material response couplings. Similarly the difference in the amplitude of vibration between cross-ply and between angle-ply configurations of LCB-2 is also caused by difference in material response couplings due to lamina stacking arrangement.

5.2.2.3. Impulsive Load

In case of impulsive load, deflection responses of various configurations of LCB-1 and LCB-2 are shown in Figs. 23 and 24 respectively. Magnitude of the applied load is P = 0.025 N.s and is applied at t = 0. Figs. 23 and 24 show that variation of deflection's magnitude, with time, follows the same trend as observed in case of harmonic and step loads i.e. cross-ply LCBs undergo small deflections as compared to angle-ply LCBs. Effect of lamina stacking arrangement can also be observed

under impulsive load. Difference in maximum amplitude of deflection and dominant vibration period, in Fig. 23, between CP1 and CP2 is due to the difference in response couplings resulting from the variation in lamina lay-up scheme. Similarly in Fig. 23, AP1 and AP2 also shows the influence of lamina lay-up scheme on the dynamic response of LCB. Difference in response between CP3-CP4 and between AP3-AP4, in Fig. 24, is also due to lamina stacking arrangement.

Non-smooth response in Figs. 23 and 24 is the aftermath of rich frequency content of Impulsive load. Vibration of a structure consists of two phases when subjected to impulsive load. Structure is under forced vibration in the first phase and it is of very small duration which starts with the application of load and finishes with the load removal. Second phase is the free vibration phase as shown in Figs. 23 and 24. Final conditions of displacement and velocity at the end of forced vibration phase serve as initial conditions for this phase. In this phase, fundamental natural frequency of vibration is dominant. It can also be observed by comparing the dominant vibration period of LCBs in Figs. 23 and 24 to deflection response plots in Figs. 11 and 13. As structure vibrates with fundamental natural frequency under step loads, it can be seen that the dominant frequency of vibration in Figs. 23 and 24 is approximately the same as vibration frequency in Figs. 11 and 13. Deflection response in Figs. 23 and 24 is highly non-smooth, as compared to response under step loads, due to the interaction between broad range of frequencies present in impulsive load and the free vibration frequency.

Lowest deflection is observed for CP1 configuration as compared to all other configurations of LCB-1 and LCB-2. Hence it will be the best choice, among the available options, for applications where only small deflections are permitted.

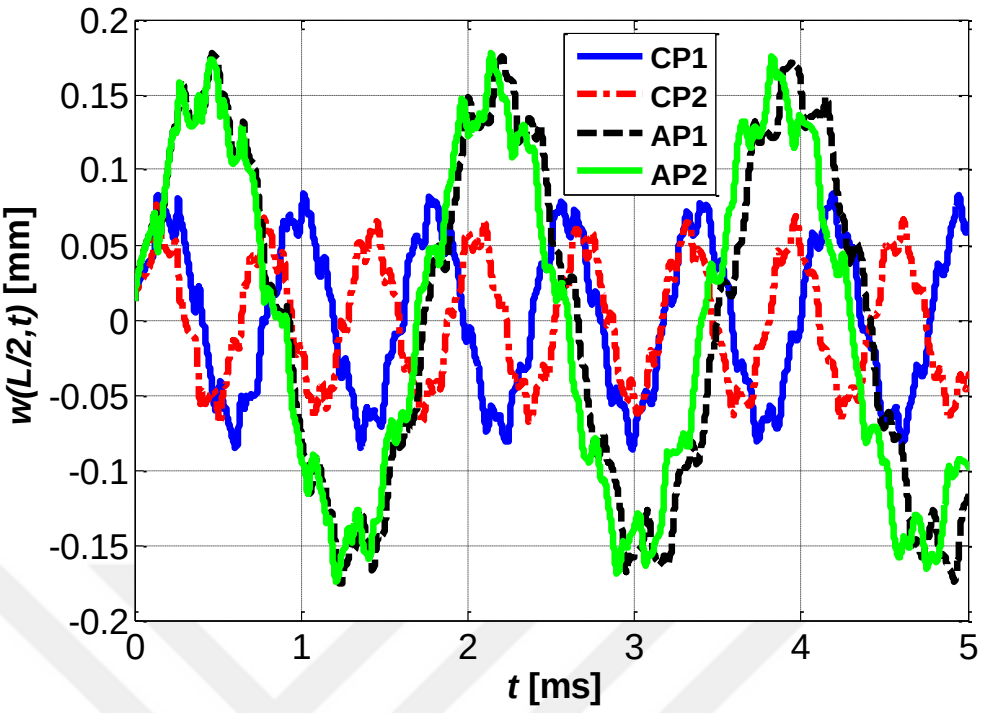

Figure 23: Deflection response LCB-1: Impulsive load $P = 0.025\text{N}\cdot\text{s}$ at x_p= L/2

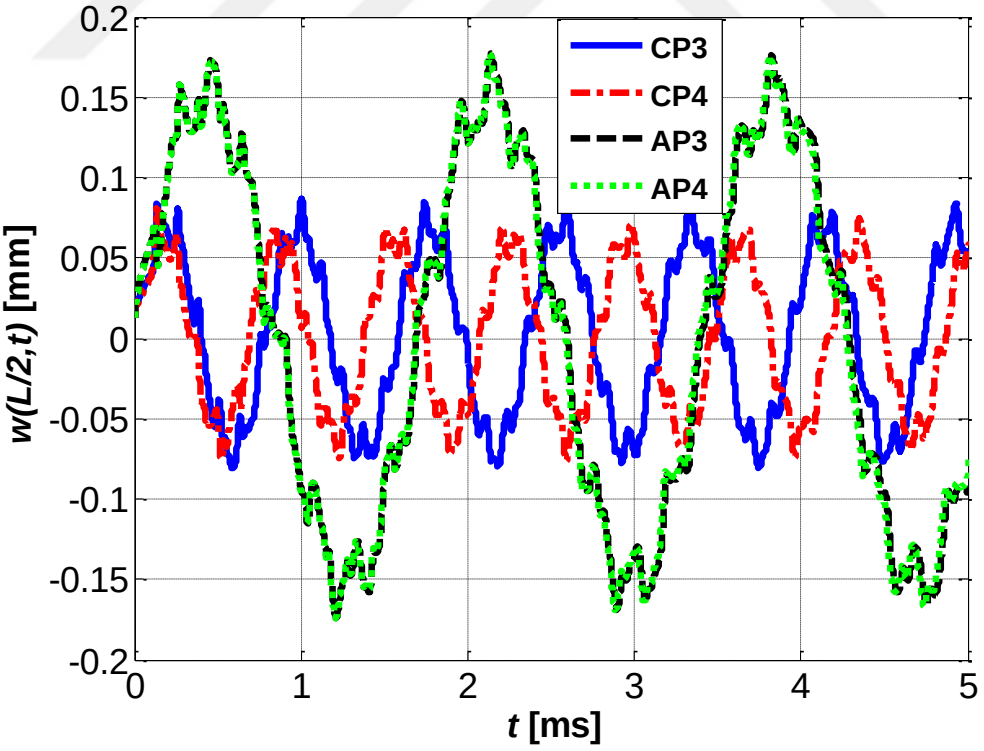

Figure 24: Deflection response LCB-2: Impulsive load $P = 0.025\text{N}\cdot\text{s}$ at x_p= L/2

Time histories of longitudinal normal stress in all configurations of LCB-1 and LCB-2 are shown in Figs. 25 and 26 respectively. In the case of impulsive load, it is observed that cross-ply configurations of LCB-1 and LCB-2 experience much larger stress values as compared to angle-ply LCBs. This is because of the fact that cross-ply configurations undergo larger twisting, bending and extensional deformations when subject to impulsive loads in comparison to step and harmonic loads. Angle-ply configurations of both LCBs experience much lower stress values and are deemed as the perfect choice for applications involving the impulsive excitations. Time histories of longitudinal stress, in Figs. 25 and 26, have very high rate of change as compared to transverse deflection. This is due to the high speed of longitudinal stress waves as compared to flexural waves.

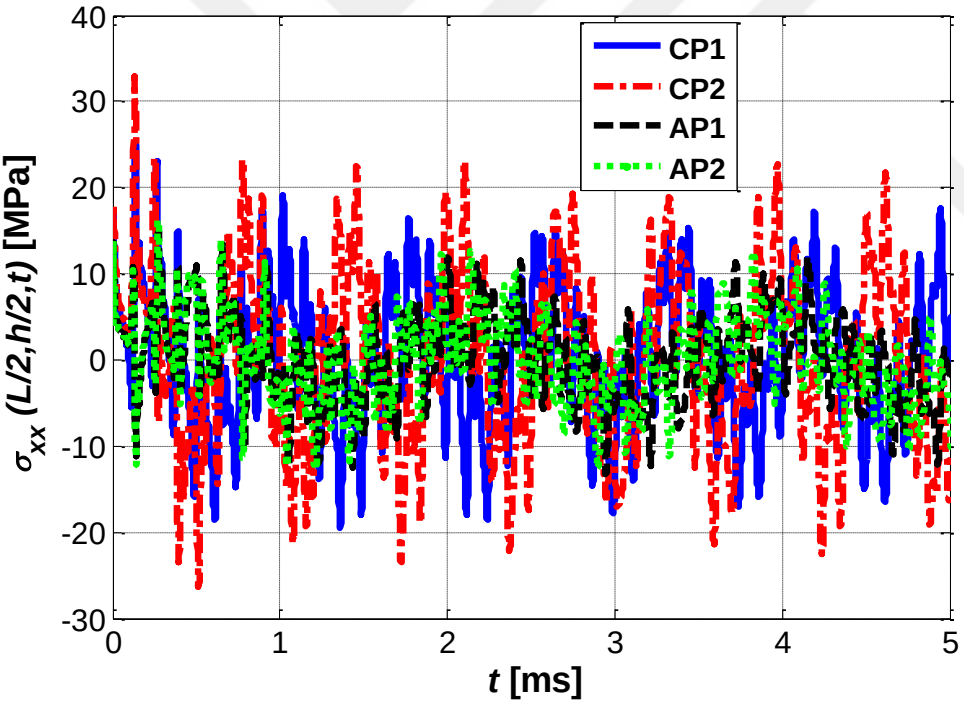

Figure 25: Longitudinal stress response LCB-1: Impulsive load $P = 0.025\text{N}\cdot\text{s}$ at x_p= L/2

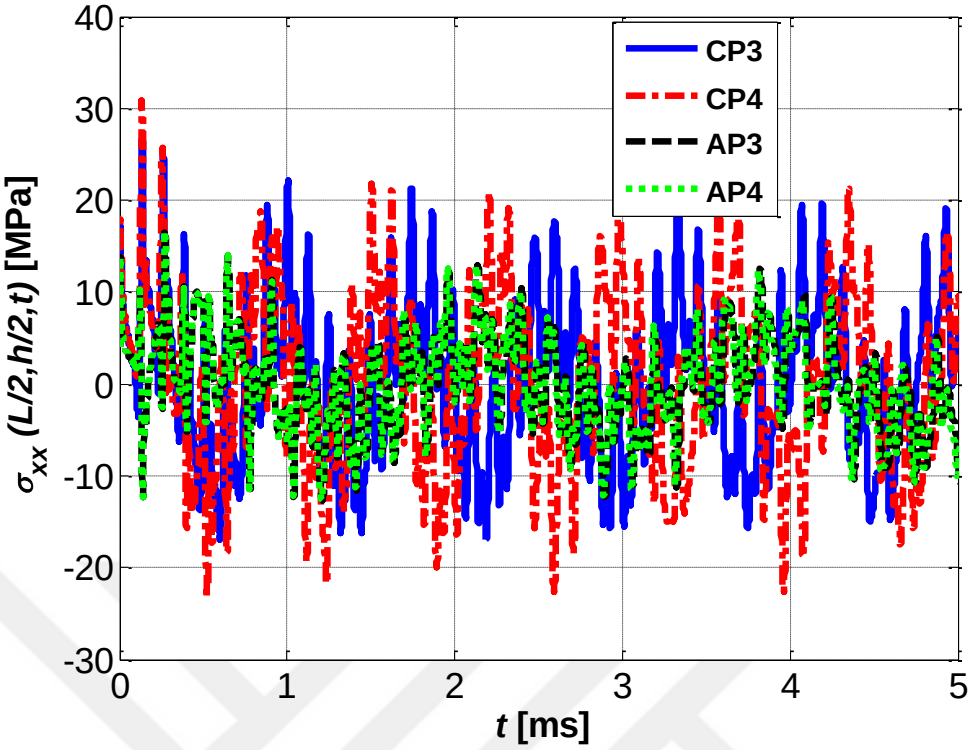

Figure 26: Longitudinal stress response LCB-2: Impulsive load $P = 0.025\text{N}\cdot\text{s}$ at x_p= L/2

CHAPTER 5

CONCLUDING REMARKS

D-BEM formulation for undamped forced vibration analysis of generally laminated composite beams is presented. Displacement field of Timoshenko beam theory is used to derive the governing equations of the problem. Material response couplings between bending, extension, twist as well as Poisson's effect and rotary inertia are included in the formulation. Weighted residual statement contains static fundamental solutions of the reduced non-homogeneous form of differential equations as weight functions. Evaluation of the weighted residual statement eventuates in the integral form of the governing equations. Domain integrals in integral formulation are evaluated by dividing the domain into cells and second degree polynomials are used as shape functions. Houbolt method is employed for solving the system of equations obtained as a result of domain discretization.

Analytical solutions for pinned-pinned beam are used as benchmarks for validating the results obtained from D-BEM. Convergence analysis is performed to find the optimum number of cells and time step for calculation of accurate time histories. It is demonstrated that a time step of 10^{-5} s and 16 cells suffice for the accurate response calculation when LCB is subjected to step or harmonic loadings. For accurate response under impulse load, 10^{-6} s is used as time step and domain is divided into 64 cells.

Two simply supported LCBs, each having four different configurations, are considered in parametric analyses. Influence of fiber angle and lamina stacking sequence is investigated on the dynamic response of LCB. It was observed that cross-ply configurations of LCB have higher fundamental vibration frequency as

compared to angle-ply LCBs and angle-ply configurations tend to have larger transverse displacements in all loading scenarios. It has been shown that variation in lamina stacking sequence results in difference in dynamic response to excitation of same type and magnitude. Stacking arrangement of laminas affects the material response couplings between extension, twist and bending, leading to different response characteristics under same excitation conditions.

It has also been observed that cross-ply configurations experience larger stress values as compared to angle-ply LCBs when subjected to impulsive load. It can be inferred that due to lower stresses in angle-ply configurations, they will be less prone to failure in comparison to the cross-ply configurations under impulsive loading of equal magnitude. In case of step and harmonic loads, magnitude of normal stress variation with time, of all configurations is generally close to each other.

The technique presented here offers a variety of options, i.e. number of plies, lamina stacking arrangement, lamina fiber angle, individual lamina thickness and materials for matrix and fibers, in the design of generally laminated composite beam for a specific application. Accurate calculation of dynamic response of LCBs, under time dependent external forces, is demonstrated. It can prove to be a promising numerical technique in design and optimization analyses of generally laminated composites due to its convergence, accuracy and stability characteristics. Extension of this technique to forced vibration studies of generally laminated composites involving damping could be an interesting area for future study.

REFERENCES

[1] J.A.M. Carrer, S.A. Fleischfresser, L.F.T. Garcia, W.J. Mansur. Dynamic analysis of Timoshenko beams by the boundary element method. Eng. Anal. Bound. Elem. 37 (2013) 1602-1616.

[2] I. Eshraghi, S. Dag. Domain-boundary element method for elastodynamics of functionally graded Timoshenko beams. Comput. Struct. 195 (2018) 113-125.

[3] G.D. Hatzigeorgiou, D.E. Beskos. Dynamic elastoplastic analysis of 3-D structures by the domain/boundary element method. Comput. Struct. 80 (2002) 339-347.

[4] C.P. Providakis, D.E. Beskos. Dynamic analysis of elasto-plastic flexural plates by the D/BEM. Eng. Anal. Bound. Elem. 14 (1994) 75-80.

[5] D. Soares Jr., J.A.M. Carrer, W.J. Mansur. Non-linear elastodynamic analysis by the BEM: an approach based on the iterative coupling of the D-BEM and TD-BEM formulations. Eng. Anal. Bound. Elem. 29 (2005) 761-774.

[6] J.A.M. Carrer, W.J. Mansur. Scalar wave equation by the boundary element method: a D-BEM approach with constant time-weighting functions. Int. J. Numer. Meth. Eng. 81 (2010) 1281-1297.

[7] J.A.M. Carrer, W.J. Mansur, R.J. Vanzuit. Scalar wave equation by the boundary element method: a D-BEM approach with non-homogeneous initial conditions. Comput. Mech. 44 (2009) 31-44.

[8] C.P. Providakis. Transient dynamic response of elastoplastic thick plates resting on Winkler-type foundation. Nonlinear Dynam. 23 (2000) 285-302

[9] R. Pettres, L.A. de Lacerda, J.A.M. Carrer. A boundary element formulation for the heat equation with dissipative and heat generation terms. Eng. Anal. Bound. Elem. 51 (2015) 191-198.

[10] P. Oyarzun, F.S. Loureiro, J.A.M. Carrer, W.J. Mansur. A time-stepping scheme based on numerical Green's functions for the domain boundary element method: the ExGA-DBEM Newmark approach. Eng. Anal. Bound. Elem. 35 (2011) 533-542.

[11] J.R. Banerjee, F.W. Williams. Free vibration of composite beams - An exact method using symbolic computation. J. Aircr. 32 (1995) 636-642.

[12] S.R. Marur, T. Kant. On the angle ply higher order beam vibrations. Comput. Mech. 40 (2007) 25-33.

[13] Li Jun, Hua Hongxing, S. Rongying. Dynamic finite element method for generally laminated composite beams. Int. J. Mech. Sci. 50 (2008) 466-480.

[14] Y. Teboub, P. Hajela. Free vibration of generally layered composite beams using symbolic computations. Compos. Struct. 33 (1995) 123-134.

[15] V. Yildirim, E. Sancaktar, E. Kiral. Comparison of the in-plane natural frequencies of symmetric cross-ply laminated beams based on the Bernoulli–Euler and Timoshenko beam theories. J. Appl. Mech. 66 (1999) 410-417.

[16] W.Q. Chen, C.F. Lv, Z.G. Bian. Elasticity solution for free vibration of laminated beams. Compos. Struct. 62 (2003) 75-82.

[17] Li Jun, Hu Xiang, Li Xiaobin. Free vibration analyses of axially loaded laminated composite beams using a unified higher-order shear deformation theory and dynamic stiffness method. Compos. Struct. 158 (2016) 308-322.

[18] D. Shao, S. Hu, Q. Wang, F. Pang. Free vibration of refined higher-order shear deformation composite laminated beams with general boundary conditions. Composites Part B 108 (2017) 75-90.

[19] Y. Yan, A. Pagani, E. Carrera. Exact solutions for free vibration analysis of laminated, box and sandwich beams by refined layer-wise theory. Compos. Struct. 175 (2017) 28-45.

[20] R.A. Jafari-T., M. Abedi, M.H. Kargarnovin, M.T. Ahmadian. An analytical approach for the free vibration analysis of generally laminated composite beams with shear effect and rotary inertia. Int. J. Mech. Sci. 65 (2012) 97-104.

[21] F.F. Çalım. Free and forced vibrations of non-uniform composite beams. Compos. Struct. 88 (2009) 413-423.

[22] H. Youzera, Sid A. Mefta, N. Challamel, A. Tounsi. Nonlinear damping and forced vibration analysis of laminated composite beams. Composites Part B 43 (2012) 1147-1154.

[23] S.P. Machado, V.H. Cortínez. Dynamic stability of thin-walled composite beams under periodic transverse excitation. J. Sound Vib. 321 (2009) 220-241.

[24] M.H. Kadivar, S.R. Mohebpour. Forced vibration of unsymmetric laminated composite beams under the action of moving loads. Compos. Sci. Technol. 58 (1998) 1675-1684.

[25] E. Bahmyari, S.R. Mohebpour, P. Malakzadeh. Vibration Analysis of inclined laminated composite beams under moving distributed masses. Shock Vib., vol. 2014, Article ID 750916, 12 pages, 2014.

[26] Y.H. Li, L. Wang, E.C. Yang. Nonlinear dynamic responses of an axially moving laminated beam subjected to both blast and thermal loads. Int. J. Nonlınear. Mech. 101 (2018) 56-67.

[27] C. Tao, Yi-M. Fu, H.L. Dai. Nonlinear dynamic analysis of fiber metal laminated beams subjected to moving loads in thermal environment. Compos. Struct. 140 (2016) 410-416.

[28] H. Hou, G. He. Static and dynamic analysis of two-layer Timoshenko composite beams by weak-form quadrature element method. Appl. Math. Model 55 (2018) 466-483.

[29] R.M. Jones. Mechanics of Composite Materials. McGraw-Hill, New York, (1975).

[30] J.C. Houbolt. A recurrence matrix solution for the dynamic response of elastic aircraft. J. Aeronaut. Sci. 17 (1950) 540-550.

[31] L.F.T. Garcia, S.F. Villaça. Introduction to the theory of elasticity. COPPE/UFRJ, 2000 [in Portuguese].

A. DOMAIN INTEGRALS

Following domain integrals are used for calculating entries of sub-matrices **P** and **S**.

$$\int_{x_1^j}^{x_3^j} I_1 u^*\left(x,\xi_k\right)\left\{\phi_1^j\left(x\right)\ddot{u}\left(x_1^j,t\right)+\phi_2^j\left(x\right)\ddot{u}\left(x_2^j,t\right)+\phi_3^j\left(x\right)\ddot{u}\left(x_3^j,t\right)\right\}dx$$

$$=\frac{I_1}{\overline{A}_{11}}\begin{bmatrix} m_1^{kj} & m_2^{kj} & m_3^{kj}\end{bmatrix}\begin{Bmatrix}\ddot{u}_1^j\\ \ddot{u}_2^j\\ \ddot{u}_3^j\end{Bmatrix} \qquad \text{A.1}$$

$$\int_{x_1^j}^{x_3^j} I_2 u^*\left(x,\xi_k\right)\left\{\phi_1^j\left(x\right)\ddot{\psi}_x\left(x_1^j,t\right)+\phi_2^j\left(x\right)\ddot{\psi}_x\left(x_2^j,t\right)+\phi_3^j\left(x\right)\ddot{\psi}_x\left(x_3^j,t\right)\right\}dx$$

$$=\frac{I_2}{\overline{A}_{11}}\begin{bmatrix} m_1^{kj} & m_2^{kj} & m_3^{kj}\end{bmatrix}\begin{Bmatrix}\ddot{\psi}_{x1}^j\\ \ddot{\psi}_{x2}^j\\ \ddot{\psi}_{x3}^j\end{Bmatrix} \qquad \text{A.2}$$

$$\int_{x_1^j}^{x_3^j} I_3 \psi_y^*\left(x,\xi_k\right)\left\{\phi_1^j\left(x\right)\ddot{\psi}_y\left(x_1^j,t\right)+\phi_2^j\left(x\right)\ddot{\psi}_y\left(x_2^j,t\right)+\phi_3^j\left(x\right)\ddot{\psi}_y\left(x_3^j,t\right)\right\}dx$$

$$=\frac{I_3}{\overline{D}_{66}}\begin{bmatrix} m_1^{kj} & m_2^{kj} & m_3^{kj}\end{bmatrix}\begin{Bmatrix}\ddot{\psi}_{y1}^j\\ \ddot{\psi}_{y2}^j\\ \ddot{\psi}_{y3}^j\end{Bmatrix} \qquad \text{A.3}$$

$$-\int_{x_1^j}^{x_3^j} \overline{A}_{55} w_{,x}^*\left(x,\xi_k\right)\left\{\phi_1^j\left(x\right)\psi_x\left(x_1^j,t\right)+\phi_2^j\left(x\right)\psi_x\left(x_2^j,t\right)+\phi_3^j\left(x\right)\psi_x\left(x_3^j,t\right)\right\}$$

$$=\begin{bmatrix} p_1^{kj} & p_2^{kj} & p_3^{kj}\end{bmatrix}\begin{Bmatrix}\psi_{x1}^j\\ \psi_{x2}^j\\ \psi_{x3}^j\end{Bmatrix} \qquad \text{A.4}$$

$$\int_{x_1^j}^{x_3^j} I_1 w^*\left(x,\xi_k\right)\left\{\phi_1^j\left(x\right)\ddot{w}\left(x_1^j,t\right)+\phi_2^j\left(x\right)\ddot{w}\left(x_2^j,t\right)+\phi_3^j\left(x\right)\ddot{w}\left(x_3^j,t\right)\right\}dx$$

$$=\frac{I_1}{\overline{A}_{55}}\begin{bmatrix} m_1^{kj} & m_2^{kj} & m_3^{kj}\end{bmatrix}\begin{Bmatrix}\ddot{w}_1^j\\ \ddot{w}_2^j\\ \ddot{w}_3^j\end{Bmatrix} \qquad \text{A.5}$$

$$\int_{x_1^j}^{x_3^j} \lambda \overline{B}_{11} \psi_x^* \left(x, \xi_k\right) \left\{ \phi_1^j \left(x\right) u\left(x_1^j, t\right) + \phi_2^j \left(x\right) u\left(x_2^j, t\right) + \phi_3^j \left(x\right) u\left(x_3^j, t\right) \right\} dx$$

$$= \frac{\lambda \overline{B}_{11}}{\overline{D}_{11}} \begin{bmatrix} \overline{m}_1^{kj} & \overline{m}_2^{kj} & \overline{m}_3^{kj} \end{bmatrix} \begin{Bmatrix} u_1^j \\ u_2^j \\ u_3^j \end{Bmatrix} \qquad \text{A.6}$$

$$\int_{x_1^j}^{x_3^j} \lambda \overline{D}_{16} \psi_x^* \left(x, \xi_k\right) \left\{ \phi_1^j \left(x\right) \psi_y\left(x_1^j, t\right) + \phi_2^j \left(x\right) \psi_y\left(x_2^j, t\right) + \phi_3^j \left(x\right) \psi_y\left(x_3^j, t\right) \right\} dx$$

$$= \frac{\lambda \overline{D}_{16}}{\overline{D}_{11}} \begin{bmatrix} \overline{m}_1^{kj} & \overline{m}_2^{kj} & \overline{m}_3^{kj} \end{bmatrix} \begin{Bmatrix} \psi_{y1}^j \\ \psi_{y2}^j \\ \psi_{y3}^j \end{Bmatrix} \qquad \text{A.7}$$

$$\int_{x_1^j}^{x_3^j} \overline{A}_{55} \psi_{x,x}^* \left(x, \xi_k\right) \left\{ \phi_1^j \left(x\right) w\left(x_1^j, t\right) + \phi_2^j \left(x\right) w\left(x_2^j, t\right) + \phi_3^j \left(x\right) w\left(x_3^j, t\right) \right\} dx$$

$$= \lambda \begin{bmatrix} \overline{p}_1^{kj} & \overline{p}_2^{kj} & \overline{p}_3^{kj} \end{bmatrix} \begin{Bmatrix} w_1^j \\ w_2^j \\ w_3^j \end{Bmatrix} \qquad \text{A.8}$$

$$\int_{x_1^j}^{x_3^j} I_2 \psi_x^* \left(x, \xi_k\right) \left\{ \phi_1^j \left(x\right) \ddot{u}\left(x_1^j, t\right) + \phi_2^j \left(x\right) \ddot{u}\left(x_2^j, t\right) + \phi_3^j \left(x\right) \ddot{u}\left(x_3^j, t\right) \right\} dx$$

$$= \frac{I_2}{\overline{D}_{11}} \begin{bmatrix} \overline{m}_1^{kj} & \overline{m}_2^{kj} & \overline{m}_3^{kj} \end{bmatrix} \begin{Bmatrix} \ddot{u}_1^j \\ \ddot{u}_2^j \\ \ddot{u}_3^j \end{Bmatrix} \qquad \text{A.9}$$

$$\int_{x_1^j}^{x_3^j} I_3 \psi_x^* \left(x, \xi_k\right) \left\{ \phi_1^j \left(x\right) \ddot{\psi}_x\left(x_1^j, t\right) + \phi_2^j \left(x\right) \ddot{\psi}_x\left(x_2^j, t\right) + \phi_3^j \left(x\right) \ddot{\psi}_x\left(x_3^j, t\right) \right\} dx$$

$$= \frac{I_3}{\overline{D}_{11}} \begin{bmatrix} \overline{m}_1^{kj} & \overline{m}_2^{kj} & \overline{m}_3^{kj} \end{bmatrix} \begin{Bmatrix} \ddot{\psi}_{x1}^j \\ \ddot{\psi}_{x2}^j \\ \ddot{\psi}_{x3}^j \end{Bmatrix} \qquad \text{A.10}$$

Integrals mentioned above result in different expressions depending on the position of source node. With respect to a cell $\Omega_j = \left[x_1^j, x_3^j \right]$, position of the source node can be classified into the following three cases.

1) $\xi_k \le x_1^j$

2) $\xi_k \equiv x_2^j$

3) $\xi_k \ge x_3^j$

For $\xi_k \le x_1^j$, evaluation of the integrals result in the following expressions

$$m_1^{kj} = \frac{\left(x_1^j - \xi_k\right)h_e}{6}, \quad m_2^{kj} = \frac{2h_e}{3}\left(x_2^j - \xi_k\right), \quad m_3^{kj} = \frac{\left(x_3^j - \xi_k\right)h_e}{6}, \tag{A.11}$$

$$p_1^{kj} = \frac{h_e}{6}, \quad p_2^{kj} = \frac{2}{3}h_e, \quad p_3^{kj} = \frac{h_e}{6}, \tag{A.12}$$

$$\begin{aligned}\overline{p}_1^{kj} &= \frac{1}{4\lambda^{3/2}h_e^2}\left\{2\sinh\left[\sqrt{\lambda}\left(x_3^j - \xi_k\right)\right] - 2\left(1+\lambda h_e^2\right)\sinh\left[\sqrt{\lambda}\left(x_1^j - \xi_k\right)\right]\right\} \\ &- \frac{1}{4\lambda h_e}\left\{3\cosh\left[\sqrt{\lambda}\left(x_1^j - \xi_k\right)\right] + \cosh\left[\sqrt{\lambda}\left(x_3^j - \xi_k\right)\right]\right\};\end{aligned} \tag{A.13}$$

$$\begin{aligned}\overline{p}_2^{kj} &= \frac{1}{\lambda^{3/2}h_e^2}\left\{\sinh\left[\sqrt{\lambda}\left(x_1^j - \xi_k\right)\right] - \sinh\left[\sqrt{\lambda}\left(x_3^j - \xi_k\right)\right]\right\} \\ &+ \frac{1}{\lambda h_e}\left\{\cosh\left[\sqrt{\lambda}\left(x_3^j - \xi_k\right)\right] + \cosh\left[\sqrt{\lambda}\left(x_1^j - \xi_k\right)\right]\right\};\end{aligned} \tag{A.14}$$

$$\begin{aligned}\overline{p}_3^{kj} &= \frac{1}{4\lambda^{3/2}h_e^2}\left\{2\left(1+\lambda h_e^2\right)\sinh\left[\sqrt{\lambda}\left(x_3^j - \xi_k\right)\right] - 2\sinh\left[\sqrt{\lambda}\left(x_1^j - \xi_k\right)\right]\right\} \\ &- \frac{1}{4\lambda h_e}\left\{\cosh\left[\sqrt{\lambda}\left(x_1^j - \xi_k\right)\right] + 3\cosh\left[\sqrt{\lambda}\left(x_3^j - \xi_k\right)\right]\right\};\end{aligned} \tag{A.15}$$

$$\begin{aligned}\overline{m}_1^{kj} &= \frac{1}{4\lambda^2 h_e^2}\left\{2\cosh\left[\sqrt{\lambda}\left(x_3^j - \xi_k\right)\right] - 2\left(1+\lambda h_e^2\right)\cosh\left[\sqrt{\lambda}\left(x_1^j - \xi_k\right)\right]\right\} \\ &- \frac{1}{4\lambda^{3/2}h_e}\left\{3\sinh\left[\sqrt{\lambda}\left(x_1^j - \xi_k\right)\right] + \sinh\left[\sqrt{\lambda}\left(x_3^j - \xi_k\right)\right]\right\};\end{aligned} \tag{A.16}$$

$$\begin{aligned}\overline{m}_2^{kj} &= \frac{1}{\lambda^2 h_e^2}\left\{\cosh\left[\sqrt{\lambda}\left(x_1^j - \xi_k\right)\right] - \cosh\left[\sqrt{\lambda}\left(x_3^j - \xi_k\right)\right]\right\} \\ &+ \frac{1}{\lambda^{3/2}h_e}\left\{\sinh\left[\sqrt{\lambda}\left(x_3^j - \xi_k\right)\right] + \sinh\left[\sqrt{\lambda}\left(x_1^j - \xi_k\right)\right]\right\};\end{aligned} \tag{A.17}$$

$$\bar{m}_3^{kj} = \frac{1}{4\lambda^2 h_e^2}\left\{2\left(1+\lambda h_e^2\right)\cosh\left[\sqrt{\lambda}\left(x_3^j-\xi_k\right)\right]-2\cosh\left[\sqrt{\lambda}\left(x_1^j-\xi_k\right)\right]\right\}$$
$$-\frac{1}{4\lambda^{3/2}h_e}\left\{\sinh\left[\sqrt{\lambda}\left(x_1^j-\xi_k\right)\right]+3\sinh\left[\sqrt{\lambda}\left(x_3^j-\xi_k\right)\right]\right\}; \quad \text{A.18}$$

Following expressions are obtained for $\xi_k \equiv x_2^j$

$$m_1^{kj} = \frac{h_e^2}{8}, \quad m_2^{kj} = \frac{h_e^2}{4}, \quad m_3^{kj} = \frac{h_e^2}{8}, \quad \text{A.19}$$

$$p_1^{kj} = -\frac{h_e}{4}, \quad p_2^{kj} = 0, \quad p_3^{kj} = \frac{h_e}{4}, \quad \text{A.20}$$

$$\bar{p}_1^{kj} = \frac{1}{2\lambda h_e}\left\{\cosh\left[\sqrt{\lambda}h_e\right]-\sqrt{\lambda}h_e\sinh\left[\sqrt{\lambda}h_e\right]-1\right\}; \quad \text{A.21}$$

$$p_2^{kj} = 0, \quad \text{A.22}$$

$$\bar{p}_3^{kj} = \frac{1}{2\lambda h_e}\left\{1+\sqrt{\lambda}h_e\sinh\left[\sqrt{\lambda}h_e\right]-\cosh\left[\sqrt{\lambda}h_e\right]\right\}; \quad \text{A.23}$$

$$\bar{m}_1^{kj} = \frac{1}{2\lambda^2 h_e^2}\left\{\left(2+\lambda h_e^2\right)\cosh\left[\sqrt{\lambda}h_e\right]-2\left[1+\sqrt{\lambda}h_e\sinh\left(\sqrt{\lambda}h_e\right)\right]\right\}; \quad \text{A.24}$$

$$\bar{m}_2^{kj} = \frac{1}{\lambda^2 h_e^2}\left\{2\left[1-\cosh\left(\sqrt{\lambda}h_e\right)+\sqrt{\lambda}h_e\sinh\left(\sqrt{\lambda}h_e\right)\right]-\lambda h_e^2\right\}; \quad \text{A.25}$$

$$\bar{m}_3^{kj} = \frac{1}{2\lambda^2 h_e^2}\left\{\left(2+\lambda h_e^2\right)\cosh\left[\sqrt{\lambda}h_e\right]-2\left[1+\sqrt{\lambda}h_e\sinh\left(\sqrt{\lambda}h_e\right)\right]\right\}; \quad \text{A.26}$$

Expressions obtained for $\xi_k \geq x_3^j$ are same in magnitude but opposite in sign to the ones found for $\xi_k \leq x_1^j$.

B. SUBMATRICES G & H

Sub-matrices **H** and **G** containing the terms pertaining to boundary nodes are given below.

$$\mathbf{H}_{uu}^{bb} = \frac{1}{2}\begin{bmatrix} 1 & -1 \\ -1 & 1 \end{bmatrix} \quad \text{B.1}$$

$$\mathbf{H}_{u\psi_x}^{bb} = \frac{\overline{B}_{11}}{2\overline{A}_{11}}\begin{bmatrix} 1 & -1 \\ -1 & 1 \end{bmatrix} \quad \text{B.2}$$

$$\mathbf{H}_{u\psi_y}^{bb} = \frac{\overline{B}_{16}}{2\overline{A}_{11}}\begin{bmatrix} 1 & -1 \\ -1 & 1 \end{bmatrix} \quad \text{B.3}$$

$$\mathbf{H}_{\psi_y u}^{bb} = \frac{\overline{B}_{16}}{2\overline{D}_{66}}\begin{bmatrix} 1 & -1 \\ -1 & 1 \end{bmatrix} \quad \text{B.4}$$

$$\mathbf{H}_{\psi_y\psi_x}^{bb} = \frac{\overline{D}_{16}}{2\overline{D}_{66}}\begin{bmatrix} 1 & -1 \\ -1 & 1 \end{bmatrix} \quad \text{B.5}$$

$$\mathbf{H}_{\psi_y\psi_y}^{bb} = \frac{1}{2}\begin{bmatrix} 1 & -1 \\ -1 & 1 \end{bmatrix} \quad \text{B.6}$$

$$\mathbf{H}_{ww}^{bb} = \frac{1}{2}\begin{bmatrix} 1 & -1 \\ -1 & 1 \end{bmatrix} \quad \text{B.7}$$

$$\mathbf{H}_{\psi_x u}^{bb} = \frac{\overline{B}_{11}}{2\overline{D}_{11}}\begin{bmatrix} 1 & -\cosh\left[\sqrt{\lambda}L\right] \\ -\cosh\left[\sqrt{\lambda}L\right] & 1 \end{bmatrix} \quad \text{B.8}$$

$$\mathbf{H}_{\psi_x\psi_x}^{bb} = \frac{1}{2}\begin{bmatrix} 1 & -\cosh\left[\sqrt{\lambda}L\right] \\ -\cosh\left[\sqrt{\lambda}L\right] & 1 \end{bmatrix} \quad \text{B.9}$$

$$\mathbf{H}_{\psi_x\psi_y}^{bb} = \frac{\overline{D}_{16}}{2\overline{D}_{11}}\begin{bmatrix} 1 & -\cosh\left[\sqrt{\lambda}L\right] \\ -\cosh\left[\sqrt{\lambda}L\right] & 1 \end{bmatrix} \quad \text{B.10}$$

$$\mathbf{H}_{\psi_x w}^{bb} = \frac{\overline{A}_{55}}{2\overline{D}_{11}\sqrt{\lambda}}\begin{bmatrix} 0 & -\sinh\left[\sqrt{\lambda}L\right] \\ \sinh\left[\sqrt{\lambda}L\right] & 0 \end{bmatrix} \quad \text{B.11}$$

$$\mathbf{G}_{uu}^{bb} = \frac{L}{2\overline{A}_{11}}\begin{bmatrix} 0 & -1 \\ 1 & 0 \end{bmatrix} \quad \text{B.12}$$

$$\mathbf{G}_{\psi_y\psi_y}^{bb} = \frac{L}{2\overline{D}_{66}}\begin{bmatrix} 0 & -1 \\ 1 & 0 \end{bmatrix} \quad \text{B.13}$$

$$\mathbf{G}_{ww}^{bb} = \frac{L}{2\overline{A}_{55}}\begin{bmatrix} 0 & -1 \\ 1 & 0 \end{bmatrix} \quad \text{B.14}$$

$$\mathbf{G}_{\psi_x\psi_x}^{bb} = \frac{1}{2\overline{D}_{11}\sqrt{\lambda}}\begin{bmatrix} 0 & -\sinh\left[\sqrt{\lambda}L\right] \\ \sinh\left[\sqrt{\lambda}L\right] & 0 \end{bmatrix} \quad \text{B.15}$$

H and **G** sub-matrices containing the terms relevant to domain nodes but independent from the domain integrals are given as follows

$$\mathbf{H}_{uu}^{db} = -\frac{1}{2}\begin{bmatrix} 1 & 1 \end{bmatrix} \quad \text{B.16}$$

$$\mathbf{H}_{u\psi_x}^{db} = -\frac{\overline{B}_{11}}{2\overline{A}_{11}}\begin{bmatrix} 1 & 1 \end{bmatrix} \quad \text{B.17}$$

$$\mathbf{H}_{u\psi_y}^{db} = -\frac{\overline{B}_{16}}{2\overline{A}_{11}}\begin{bmatrix} 1 & 1 \end{bmatrix} \quad \text{B.18}$$

$$\mathbf{H}_{u\psi_x}^{dd} = \frac{\overline{B}_{11}}{\overline{A}_{11}}\mathbf{I} \quad \text{B.19}$$

$$\mathbf{H}_{u\psi_y}^{dd} = \frac{\overline{B}_{16}}{\overline{A}_{11}}\mathbf{I} \quad \text{B.20}$$

$$\mathbf{H}_{\psi_x\psi_x}^{db} = -\frac{1}{2}\left[\cosh\left[\sqrt{\lambda}\left(\xi_k\right)\right] \quad \cosh\left[\sqrt{\lambda}\left(L-\xi_k\right)\right]\right] \quad \text{B.21}$$

$$\mathbf{H}_{\psi_x u}^{db} = -\frac{\overline{B}_{11}}{2\overline{D}_{11}}\left[\cosh\left[\sqrt{\lambda}(\xi_k)\right] \quad \cosh\left[\sqrt{\lambda}(L-\xi_k)\right]\right] \quad \text{B.22}$$

$$\mathbf{H}_{\psi_x\psi_y}^{db} = -\frac{\overline{D}_{16}}{2\overline{D}_{11}}\left[\cosh\left[\sqrt{\lambda}(\xi_k)\right] \quad \cosh\left[\sqrt{\lambda}(L-\xi_k)\right]\right] \quad \text{B.23}$$

$$\mathbf{H}_{\psi_x w}^{db} = \frac{\overline{A}_{55}}{2\overline{D}_{11}\sqrt{\lambda}}\left[\sinh\left[\sqrt{\lambda}(\xi_k)\right] \quad -\sinh\left[\sqrt{\lambda}(L-\xi_k)\right]\right] \quad \text{B.24}$$

$$\mathbf{H}^{dd}_{\psi_x u} = \frac{\overline{B}_{11}}{\overline{D}_{11}}\mathbf{I} \quad \text{B.25}$$

$$\mathbf{H}^{dd}_{\psi_x \psi_y} = \frac{\overline{D}_{16}}{\overline{D}_{11}}\mathbf{I} \quad \text{B.26}$$

$$\mathbf{H}^{db}_{\psi_y \psi_y} = -\frac{1}{2}[1 \quad 1] \quad \text{B.27}$$

$$\mathbf{H}^{db}_{\psi_y u} = -\frac{\overline{B}_{16}}{2\overline{D}_{66}}[1 \quad 1] \quad \text{B.28}$$

$$\mathbf{H}^{db}_{\psi_y \psi_x} = -\frac{\overline{D}_{16}}{2\overline{D}_{66}}[1 \quad 1] \quad \text{B.29}$$

$$\mathbf{H}^{dd}_{\psi_y u} = \frac{\overline{B}_{16}}{\overline{D}_{66}}\mathbf{I} \quad \text{B.30}$$

$$\mathbf{H}^{dd}_{\psi_y \psi_x} = \frac{\overline{D}_{16}}{\overline{D}_{66}}\mathbf{I} \quad \text{B.31}$$

$$\mathbf{H}^{db}_{ww} = -\frac{1}{2}[1 \quad 1] \quad \text{B.32}$$

$$\mathbf{G}^{db}_{uu} = \frac{1}{2\overline{A}_{11}}\left[\xi_k \quad -(L-\xi_k)\right] \quad \text{B.33}$$

$$\mathbf{G}^{db}_{\psi_y \psi_y} = \frac{1}{2\overline{D}_{66}}\left[\xi_k \quad -(L-\xi_k)\right] \quad \text{B.34}$$

$$\mathbf{G}^{db}_{ww} = \frac{1}{2\overline{A}_{55}}\left[\xi_k \quad -(L-\xi_k)\right] \quad \text{B.35}$$

$$\mathbf{G}^{db}_{\psi_x \psi_x} = \frac{1}{2\overline{D}_{11}\sqrt{\lambda}}\left[\sinh\left[\sqrt{\lambda}(\xi_k)\right] \quad -\sinh\left[\sqrt{\lambda}(L-\xi_k)\right]\right] \quad \text{B.36}$$